Neuropsychol Rev (2015) 25:250–271
DOI 10.1007/s11065-015-9291-z

REVIEW

Diffusion MRI and its Role in Neuropsychology

Bryon A. Mueller[1] · **Kelvin O. Lim**[1,2] · **Laura Hemmy**[1,2] · **Jazmin Camchong**[1]

Received: 4 June 2015 / Accepted: 21 July 2015 / Published online: 9 August 2015

Abstract Diffusion Magnetic Resonance Imaging (dMRI) is a popular method used by neuroscientists to uncover unique information about the structural connections within the brain. dMRI is a non-invasive imaging methodology in which image contrast is based on the diffusion of water molecules in tissue. While applicable to many tissues in the body, this review focuses exclusively on the use of dMRI to examine white matter in the brain. In this review, we begin with a definition of diffusion and how diffusion is measured with MRI. Next we introduce the diffusion tensor model, the predominant model used in dMRI. We then describe acquisition issues related to acquisition parameters and scanner hardware and software. Sources of artifacts are then discussed, followed by a brief review of analysis approaches. We provide an overview of the limitations of the traditional diffusion tensor model, and highlight several more sophisticated non-tensor models that better describe the complex architecture of the brain's white matter. We then touch on reliability and validity issues of diffusion measurements. Finally, we describe examples of ways in which dMRI has been applied to studies of brain disorders and how identified alterations relate to symptomatology and cognition.

Keywords Diffusion · Magnetic resonance imaging · Diffusion tensor imaging · Neuroimaging · Reliability · Validity · Neuropsychology

✉ Jazmin Camchong
camch002@umn.edu

[1] Department of Psychiatry, Medical School, University of Minnesota, 717 Delaware St SE, Suite 516, Minneapolis, MN 55414, USA

[2] Minneapolis VA Health Care System, Minneapolis, MN, USA

Introduction

A strength of Magnetic Resonance Imaging (MRI) is the great number of tissue contrasts that can be created through the design of the acquisition sequence and selection of parameters. Examples of tissue contrasts include T_1 contrast that is used for anatomical imaging and T_2* for functional imaging. The ability to measure molecular diffusion of water in tissues gave rise to diffusion MRI (dMRI). While applicable in many tissues including kidney and muscle, this review will focus exclusively on the use of dMRI as a non-invasive imaging technique that can be used to examine white matter pathways in the brain. dMRI is one of the key technologies included in the NIH (National Institutes of Health) Human Connectome Project, used for mapping anatomical connections in the living human brain through the use of tractography.

In this review, we begin with a definition of diffusion and how diffusion is measured with MRI. Next we introduce the diffusion tensor model, the predominant model used in dMRI. We then describe acquisition issues related to acquisition parameters and scanner hardware and software. Next, we provide a brief review of analysis approaches followed by a section on potential artifacts. Several non-tensor models are introduced. We then touch on measurement reliability and validity issues. Finally we provide examples of ways in which dMRI has been applied to studies of brain disorders and how identified alterations relate to symptomatology and cognition.

Diffusion Measurement with MRI

Diffusion magnetic resonance imaging is a type of MRI in which image contrast is based on the diffusion of water molecules in tissue. dMRI is a non-invasive method that does not require any type of exogenous contrast agent. While a

complete description of the physics of diffusion is beyond the scope of this review, these can be found in several review articles in the literature (Beaulieu 2002; Le Bihan 2003).

Diffusion is the random motion of molecules due to kinetic energy. This motion, which is often referred to as "Brownian" motion after the botanist Robert Brown, was well described by Albert Einstein (Einstein 1926). Since diffusion is a random process, it is not possible to predict the motion of a single molecule. However, in a free medium the translation probability distribution of a molecule is well described using a 3 dimensional Gaussian distribution.

In the 1960s it was discovered that magnetic resonance is particularly well suited to the quantitative measurement of diffusion (Stejskal and Tanner 1965). By adding a pair of magnetic field gradient pulses with equal magnitude on either side of the refocusing RF pulse of a spin echo pulse MRI sequence, Stejskal & Tanner (Stejskal and Tanner 1965) enabled the measurement of diffusion of water molecules, albeit in one direction at a time. To measure the diffusion of water along a specific direction (e.g. x), a magnetic field gradient is applied along this direction of interest (e.g. x). This magnetic field gradient labels the location of the water molecules along the gradient direction. After a short delay a second magnetic field gradient is applied with the same amplitude and in the same direction as the first gradient. Water motion along the direction of the applied gradients, between the applications of the pair of gradients, leads to an attenuation of the MR signal from the collection of water molecules in each voxel, and the magnitude of the signal loss is used to calculate the apparent diffusion coefficient.

Even though this concept was described in 1965, the measurement of diffusion using MR was not developed into an imaging modality until the mid 1980s, when LeBihan and colleagues showed that diffusion measurements could be made using a clinical scanner (LeBihan 1990). Due to long imaging times, however, subject movement artifacts made these measurements very difficult. The development of echo-planar imaging (EPI) which enabled a single slice to be imaged in 100 msec, largely solved the intra measurement movement problem (Beaulieu et al. 1993). In a medium without barriers and in the absence of flow, mean displacement across all water molecules is zero but the mean square of the displacement is non-zero, proportional to time, with the proportionality constant (the diffusion coefficient D) dependent on molecular weight, viscosity, and temperature. In areas without barriers, such as cerebral spinal fluid (CSF) in the brain, the diffusion coefficient is about 3×10^{-3} mm^2/s and the order of magnitude distance water molecules diffuse during the diffusion encoding of the sequences is 10 μm. In tissue, however, water diffusion is hindered or restricted by the various barriers created by the cellular microstructure (Fig. 1). Such structures are typically smaller than the characteristic distances traveled by water molecules during diffusion imaging. For example, axons in the human corpus callosum have a median diameter of 0.6–1.0 μm with a range from 0.2 to 10 μm (Aboitiz et al. 1992). Interactions with cellular structures will tend to reduce the mean distance traveled by water molecules compared to the intrinsic diffusion of Brownian

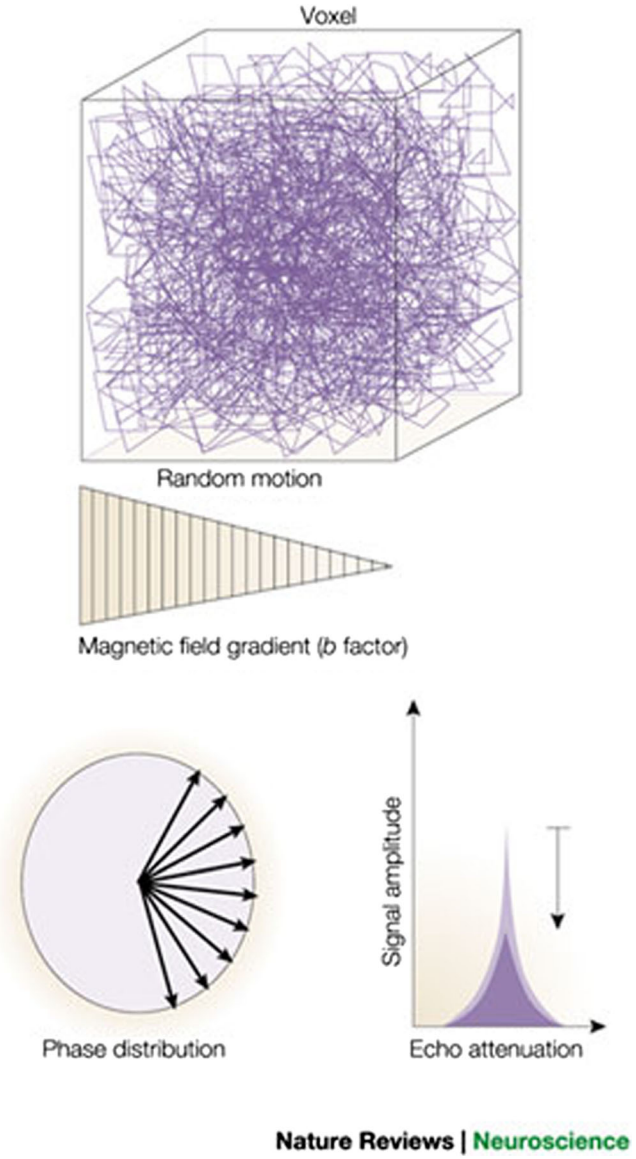

Fig. 1 Principles of diffusion magnetic resonance imaging (dMRI) from Le Bihan 2003. In the presence of a spatially varying magnetic field (induced through a magnetic field gradient, the amplitude and timing of which are characterized by a 'b' factor), moving molecules emit radiofrequency signals with slightly different phases. In a small volume (voxel) containing a large number of diffusing molecules, these phases become randomly distributed, directly reflecting the trajectory of individual molecules (that is, the diffusion process). This diffusion-related phase distribution of the signal results in an attenuation of the MRI signal. This attenuation (A) quantitatively depends on the gradient characteristics (embedded in the b factor) and the diffusion coefficient (D), according to $A = e^{-bD}$. As diffusion effects are small, large gradient intensities must be used, which requires special MRI hardware (reprinted from (Le Bihan 2003) with permission)

motion. To indicate that dMRI is sensitive to effects beyond Brownian motion (cellular interactions, flow and other biological processes), the diffusion measured in dMRI is referred to as the apparent diffusion coefficient (ADC). Indeed, dMRI is sensitive to tissue microstructure specifically because it is a measurement of the voxel by voxel deviation in from that of the intrinsic Brownian diffusivity of water.

Diffusion Tensor Model

If the diffusion is the same in all directions (isotropic) then making a single measurement, in a single arbitrary direction is sufficient to measure the diffusion of the sample. However, in the case where diffusion may be influenced by the environment, such as by highly organized structures of white matter fibers, then the measured diffusion is dependent on the direction, making the diffusion anisotropic. A new model which allowed for the measurement of anisotropic diffusion was needed to better describe the imaging results and by extension the underlying microstructure. Basser et al. (1994) introduced the *diffusion tensor model* in 1994. Since the tensor model contains six free parameters, a minimum of six volumes with linearly independent diffusion encoding gradients are needed to apply the tensor model, although the collection of more than six directions is desirable as more directions lead to improved precision and accuracy of the resultant diffusion tensor. The tensor model parametrizes the diffusion in each voxel with an ellipsoid, the mathematical description of an egg shaped object (Fig. 2). The major axis of the ellipsoid (ε_1) points in the direction of the maximum diffusivity (λ_1) of that voxel. The direction of maximum diffusion is usually assumed point in the direction of the major fiber tract in the voxel. The diffusivities along the medium (ε_2) and minor (ε_3) axes of the diffusion ellipsoid, which are perpendicular to the main fiber orientation, are also computed (λ_2,λ_3) in the tensor analysis. The introduction of the diffusion tensor model was crucial because it allowed a rotationally invariant description of the shape of water diffusion; before the introduction of the tensor model the diffusivity was only determined along the direction of the diffusion encoding direction used for each diffusion volume collected (Moseley et al. 1990; O'Donnell and Westin 2011). This improved modeling is much better suited for the examination of complex white matter tracts in the human brain.

The three diffusion values computed along the axes of the diffusion ellipsoid are rotationally invariant, meaning the same diffusion values are computed independent of the orientation of the brain in the scanner. Several numeric (or scalar) diffusion metrics are often computed from the three diffusion values ($\lambda_1, \lambda_2, \lambda_3$) derived from the tensor model (Le Bihan et al. 2001) (Table 1). These include three diffusivity metrics: the axial diffusivity (AD = λ_1) which is the maximum diffusivity in the voxel (often interpreted as the diffusion along the primary fiber tract), the radial diffusivity (RD = $(\lambda_2 + \lambda_3)/2$) average of the diffusivities in the axes perpendicular to the major axis, and mean diffusivity (MD = $(\lambda_1 + \lambda_2 + \lambda_3)/3$) which is the average of the diffusivity values of the three axes of the diffusion ellipsoid. A fourth commonly used diffusion metric is fractional anisotropy (FA), which parametrizes the degree to which the diffusion ellipsoid deviates from spherical:

$$FA = \sqrt{\frac{3}{2}} \sqrt{\frac{(\lambda_1 - \bar{\lambda})^2 + (\lambda_2 - \bar{\lambda})^2 + (\lambda_3 - \bar{\lambda})^2}{\lambda_1^2 + \lambda_2^2 + \lambda_3^2}}$$

In addition to scalar metrics, information information about the voxel microstructure is contained in the directional information contained in the diffusion tensor ellipsoid. In voxels with high fractional anisotropy the direction of maximum diffusion is often assumed to be parallel to the major fiber bundle in the voxel. Combining the scalar and directional information from adjacent voxels can allow for the parcellation of fiber tracts in white matter and is the basis for diffusion tractography.

Acquisition Issues

The specific capabilities of the hardware and software limit the types of dMRI studies that are possible on a given scanner. Performance capabilities that impact dMRI data quality include but are not limited to magnetic field strength, maximum gradient slew rate, maximum gradient field magnitude, system signal to noise, head coil channel count, and software options. Gradient slew rate capabilities limit both how quickly the diffusion encoding gradient reaches maximum value and how fast the imaging readout can take place. The rapidly changing magnetic fields produced by the gradient coils during the diffusion encoding and echo planar readout can induce electric fields in the body of the subject. These electric fields can cause stimulation of the peripheral nerves in the subject, leading to rhythmic twitching or a vibration sensation in some subjects. While MRI scanners are designed to prevent peripheral nerve stimulation (PNS) that is a danger to the subject, PNS can be annoying or uncomfortable to the subject and hence is to be avoided. MRI scanner manufacturers and the FDA (Food and Drug Administration) have set gradient ramp rate limits such that scan protocols that are stimulating to most people cannot be created.

The selection of acquisition parameters can have a large impact on the resulting data. A partial list would include: voxel size (partial voluming), b value, smoothing, TR (repetition time, or the time starting at the application of an

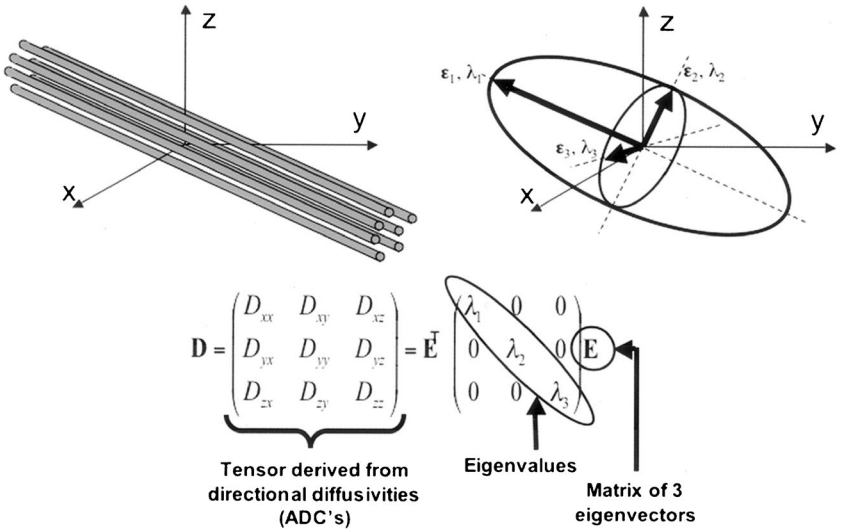

Fig. 2 Tensor matrix illustrated by Jellison et al. 2004: Top left, Fiber tracts have an arbitrary orientation with respect to scanner geometry (x, y, z axes) and impose directional dependence (anisotropy) on diffusion measurements. Top right, The three-dimensional diffusivity is modeled as an ellipsoid whose orientation is characterized by three eigenvectors (1, 2, 3) and whose shape is characterized three eigenvalues (1, 2, 3). The eigenvectors represent the major, medium, and minor principal axes of the ellipsoid, and the eigenvalues represent the diffusivities in these three directions, respectively. Bottom, This ellipsoid model is fitted to a set of at least six noncollinear diffusion measurements by solving a set of matrix equations involving the diffusivities (apparent diffusion coefficient, ADC) and requiring a procedure known as matrix diagonalization. The major eigenvector (that eigenvector associated with the largest of the three eigenvalues) reflects the direction of maximum diffusivity, which, in turn, reflects the orientation of fiber tracts. Superscript T indicates the matrix transpose (reprinted from (Jellison et al. 2004) with permission)

excitation pulse to the application of the next excitation pulse), TE (echo time, or the time between application of radiofrequency excitation pulse and the peak of the signal induced in the coil), partial fourier, parallel imaging, bandwidth, scanner software version and hardware changes. Thus, it is best to keep all aspects of the acquisition constant throughout a study. Software updates can introduce unexpected changes in acquisition parameters where default sequence parameters changes might occur. Hardware upgrades and updates can also impact data. One approach to prevent systematic differences in acquisition parameters within a study is to collect the data contemporaneously across groups that are being compared. Multi-site studies and studies that use scanners of different models and manufacturers can also complicate data comparability. Many of the approaches proposed for multi-site fMRI studies are also applicable to dMRI (Glover et al. 2012).

Artifacts

Diffusion MRI is impacted by many sources of artifacts (Jones and Cercignani 2010). These artifacts can be grouped in several different types based on their causes: artifacts caused by the scanner software and hardware, artifacts caused by the subject, and artifacts introduced into the data during processing and analysis. The aim here is not to provide an exhaustive listing of every possible artifact found in diffusion imaging but rather to point out the most common artifacts observed.

Table 1 Diffusion Metrics

dMRI Metrics	Brief Description	Common Interpretation	Known Limitations
Axial diffusivity (AD)	Diffusivity in the direction of maximum diffusion in the voxel.	Sensitive to axonal injury (Budde et al. 2009)	In voxels with crossing fibers, axonal loss in one fiber tract can lead to increased AD.
Radial diffusivity (RD)	Average of the diffusivities in the axes perpendicular to the major axis of diffusion.	Sensitive to myelin loss (Song et al. 2002)	Voxels containing crossing fibers will have high RD.
Mean diffusivity (MD)	Average of the diffusivity values of the three axes of the diffusion ellipsoid.	Sensitive to cellularity, edema, and necrosis (Alexander et al. 2007)	Large variability in measurement. Detection power depends on whether observed voxel has several crossing fibers or a single fiber (Vos et al. 2012).
Fractional anisotropy (FA)	Parameter describing how elongated (or egg shaped) the diffusion tensor ellipsoid is.	Sensitive to a wide range of pathologies	Voxels containing crossing fibers with high integrity can have low fractional anisotropy

dMRI studies typically cover the entire brain and include dozens to a hundred complete volumes with varying diffusion encoding directions per study. DWI has fairly low signal to noise and is very susceptible to motion. To reduce the effects of subject motion and to keep the studies to clinically viable times of 5–20 min, dMRI studies use very fast imaging methods. Because rapid imaging methods are required, compromises are made which can lead to a reduction of image quality and geometric fidelity.

While several imaging techniques have been used in dMRI (e.g. Line Scan Diffusion Imaging (Gudbjartsson et al. 1996), Stimulated Echo Acquisition Mode (Nolte et al. 2000), Fast Spin Echo (Pipe et al. 2002), and spiral (Lee et al. 1995)), the vast majority of studies use EPI. We will limit our discussion to common artifacts found using an EPI readout.

B0/Susceptibility

As with other EPI based image modalities (i.e. fMRI and arterial spin labeling - ASL), dMRI is sensitive to distortion and signal dropout caused by inhomogeneity in the static magnetic field of the volume being imaged. Signal dropout occurs in regions where the magnetic field is inhomogeneous within a voxel causing the magnetic spins in the voxel to dephase to the point where the signal cancels within the voxel. Distortion occurs because the expected mapping of phase accumulation to position is incorrect due to magnetic field inhomogeneity. This typically occurs in regions of high susceptibility at air-tissue boundaries such as the medial inferior frontal lobe above the sinus and temporal poles near the ear canals.

Head Motion

Head motion is a major source of artifact in dMRI and multiple approaches should be taken to avoid or reduce the effect of motion in dMRI. The most important approach is to prevent as much motion as possible. Be sure the subject is as comfortable as possible, instructing the subject to remain as still as possible, warning the subject about the noise and vibration that will occur during the diffusion imaging. The use of comfortable padding around the head that helps restrict head motion can be helpful. Also keep the imaging time as short as possible.

Even with the use of optimal acquisition methods, however, some subjects will move during a study. Such motion can be classified into three categories: motion that occurs between volumes in the acquisition, motion that occurs within the acquisition of a volume, and motion that occurs within the acquisition of a single slice. Slow scale motion over the course of minutes that occurs between volumes over the dMRI acquisition will lead to between volume misregistration throughout the dMRI time series and artifacts in the tensor computation. To prevent such artifacts image processing pipelines that include motion corrections/registration should always be used with dMRI. Head motion that occurs over the seconds it takes to acquire a single diffusion volume can lead to a misregistration of the slices within the volume, particularly if an interleaved slice acquisition is used (Fig. 3). Fast head motion that occurs during the acquisition of a single diffusion slice can lead to the artifactual reduction or even even complete disappearance of signal in part or all of one or more slices in a volume (Fig. 4). While most traditional dMRI processing pipelines apply motion correction as a processing step, many do not apply methods that correct for within volume slice misregistration or motion induced signal loss in a slice. Approaches that can be used to reduce artifacts in these cases include removing affected volumes before processing or the use of methods to detect outlier voxels, slices or volumes and then use interpolation methods to estimate the signal or use robust methods to de-weight the contribution of the artifactual voxels in the computation of the tensor (Chang et al. 2005; Dubois et al. 2014).

Spiking

EPI based dMRI methods are particularly stressful on the scanner hardware due to the fast switching times, high gradient amplitudes and gradient switching induced vibrations that occur during the imaging. Spike noise is usually caused by a hardware problem that causes the scanner readout electronics to register an erroneously large signal during the scan. When the scanner reconstruction system creates the image, the spike can result in wavy or "corduroy" patterns in the image. The exact frequency, angle and intensity of the wavy pattern will depend on when the spike(s) occur during the image acquisition. Although scanner hardware has improved greatly over the past 20 years, spike noise remains a sporadic source of image artifact on many MRI systems. Spike noise can seriously impact image quality of the affected slices. The best approach to prevent spike noise is by insuring the scanner is working properly through a robust quality assurance program. The service engineer should be notified immediately when spiking is observed to insure the problem is rectified. For this reason good dMRI practice includes evaluating image quality during data acquisition and including automated QA (quality assurance) methods that evaluate dMRI images for spike noise. For data that contain spikes, the options depend on the severity of the problem, from excluding the subject data to rejecting whole volumes or using interpolation methods to replace corrupted slices using interpolation from similar volumes (Chavez et al. 2009).

Vibration

The ramping of the strong diffusion gradients used to create diffusion weighting causes large, periodic mechanical stresses on the gradient hardware. These stresses lead to acoustic noise

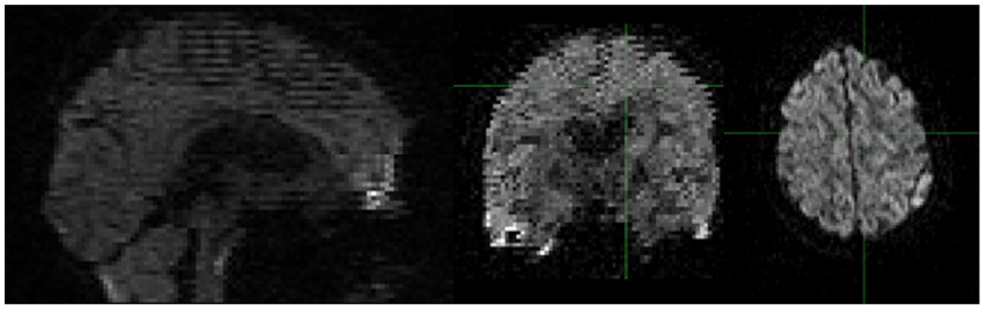

Fig. 3 Illustration of the effect of subject motion during the acquisition of a dMRI volume. Slices were acquired using an interleaved acquisition, in which the odd slices were acquired sequentially followed by the even slices. A clear stair step pattern is seen in the sagittal and coronal views due to motion between the first (*odd slices*) and second (*even slices*) parts of the acquisition. In the axial projection the slices appear unaffected by the motion

and vibration in the gradients. The mechanical vibration of the gradients can be transmitted through the patient table to the subject's brain (Gallichan et al. 2010). The amplitude of the table vibration will have a complex dependence on the direction of the diffusion sensing gradient, the details of the magnet design, and subject and sequence parameters. Understanding the symptoms of vibrational artifacts and checking the data for these effects is important in dMRI. Methods have been developed to automatically check for and correct such artifacts and should be considered (Gallichan et al. 2010; Mohammadi et al. 2012).

Eddy Currents

An eddy current is a transient electrical current created in the conducting structures of the magnet by the changes in the magnetic field gradients. Echo planar diffusion imaging is particularly prone to eddy-current artifacts because of the

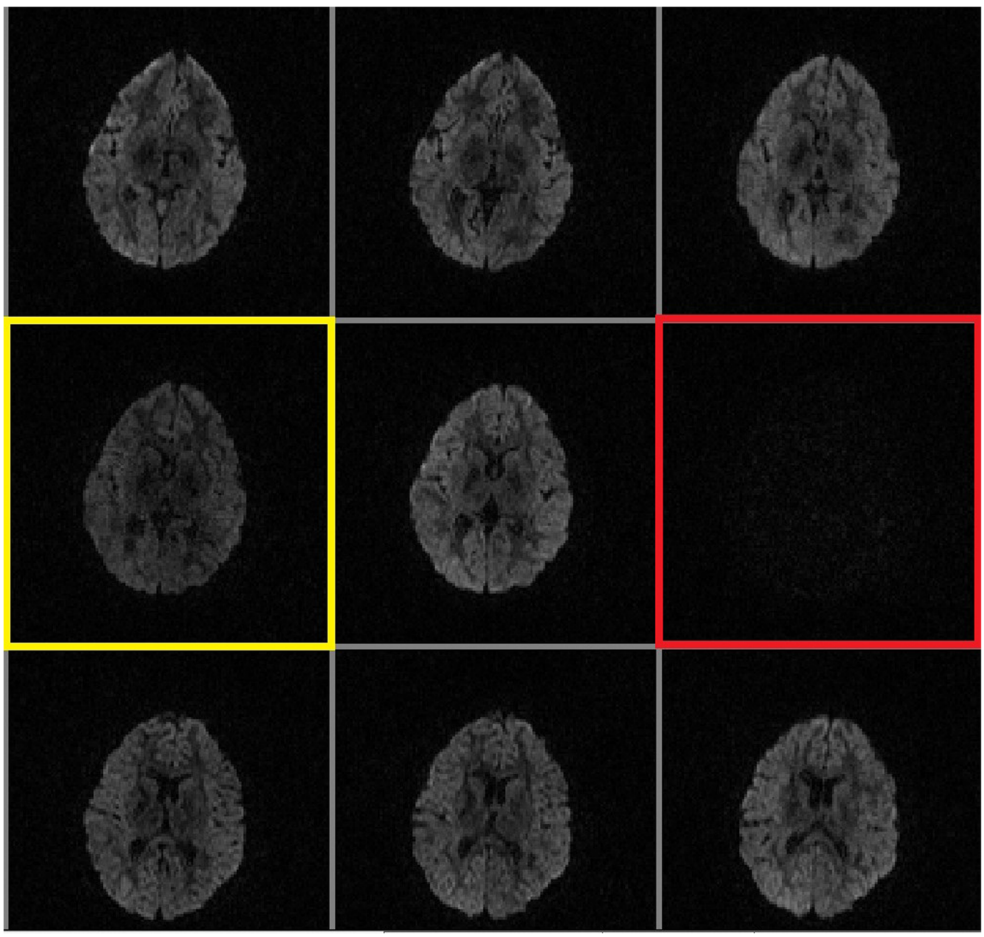

Fig. 4 Illustration of the effect of fast individual subject motion on dMRI data. Nine spatially consecutive slices are shown from one volume of an interleaved type dMRI acquisition. One slice (*red box*) has a near absence of signal while a second slice (*yellow box*) shows a more subtle signal reduction. This artifact was caused by fast subject motion over the several hundred milliseconds it took to acquire the red and yellow slices, which were acquired sequentially in time

relatively long EPI readouts combined with strong diffusion gradients which are switched rapidly. Unlike the distortions created by main field inhomogeneities, eddy currents effects are dependent on the strength and direction of the diffusion encoding gradient. These eddy currents cause translation, stretching and shearing distortions in the phase encoding direction of the image, depending on the direction of the gradient.

Eddy current distortions lead to gradient direction dependent spatial misregistration between the different diffusion-encoding directions and the images collected without diffusion encoding. Eddy current distortions are typically corrected using a twelve degree of freedom affine registration of the 4D volume to the image collected without diffusion encoding, simultaneously correcting the data for subject motion. Such methods work reasonably well for data collected with the moderate b values of about 1000 s/mm^2 used in most studies. At b values greater than 1000 s/mm^2, these methods may fail due to the lack of signal intensity needed to perform the necessary registrations.

Analysis Approaches

Once collected, the diffusion imaging data is typically run through a series of processing steps, or processing pipeline, with the final goal being the generation of one or more diffusion metrics that can that be used to investigate possible group differences between populations or in a correlation analysis with cognitive metrics. The analysis pipeline will usually have 3 major sections, data preprocessing (eddy current correction, motion correction, and brain extraction), computation of the diffusion tensor and scalar maps, and quantitative analysis. There are a large number of software packages available to perform diffusion and other MRI analysis; many such packages are found on The Neuroimaging Informatics Tools and Resources Clearinghouse webpage (NITRC, https://www.nitrc.org/).

The goal of most dMRI studies is to compare DTI metrics between two or more subject populations or investigate correlations between DTI metrics and relevant cognitive measures. DTI metrics commonly used in such analyses include mean diffusivity (MD), axial diffusivity (AD), radial diffusivity (RD), fractional anisotropy (FA) (Fig. 5). Many methods have been used for preparing the individual diffusion data for statistical group comparison or correlations analysis. The various methods share a common goal of extracting summary measures for statistical comparison, with the differences being how they go about identifying common anatomical areas across subjects for comparison. The method most appropriate for a given study will depend on the questions the study is trying to answer.

Region of Interest

A region of interest (ROI) approach is often used when the study has hypotheses involving specific brain regions of interest or pathways. A histogram approach can be used when white matter integrity alterations are thought to be diffuse across the brain. Voxel based morphometry (VBM) allows for a voxel by voxel comparison by transforming the scalar maps into a common template space and then applying statistical analyses on the imaging data. By including the directional information from the tensor, diffusion tractography based methods allow for several types of analyses including ROI definition based on specific white matter tracts but also novel metrics associated with connectivity between brain regions.

ROI analysis is based on the manual delineation of specific regions of the brain or on an automatic parcellation method. The shape of the ROI can either follow the shape of an anatomic structure (i.e. corpus callosum, internal capsule, etc) or have a geometric shape (i.e. spherical, cubical, etc). Ideally, ROIs are determined on imaging data (T_1) independent from the DTI data and then registered onto the diffusion parametric map to avoid position bias. Summary statistics (i.e. mean, standard deviation, etc) from the DTI scalar map of interest (i.e. FA, MD, etc) is then computed across subjects. Statistical analysis can then be performed on the resulting values.

Manually placed ROIs have been used in many studies. The main advantage to manual ROI methods are the high sensitivity to small changes in DTI values in focal, hypothesized parts of the brain. Use of manually placed ROIs has several disadvantages, however, including that the method is labor intensive, requires significant anatomic knowledge, requires a clear a priori hypothesis that specific brain regions are of interest, can have low intra- and inter- rater reliability and can have the difficulty of precise registration of the anatomic data to the diffusion data. These disadvantages notwithstanding, manual ROI methods can be useful for studies with moderate sized subject groups and specific hypothesis of subtle changes in small, well defined brain regions, although the use of manually placed ROIs is much less common today than 5 or 10 years ago.

Automated methods for ROI definition can be performed using parcellation of anatomic data and then transfer of the ROI onto the diffusion data or through the registration of DTI data onto a template space with the application of a common ROI based on anatomic information (i.e. specific tracks from the JHU [John Hopkins University] atlas; (Hua et al. 2008)). Automated ROI methods have the advantage that they require less labor, the ROI selection rules will be consistently applied, and the method can be scaled to studies with large subject numbers. The disadvantage is that ROI placement accuracy should be confirmed for every subject to ensure that the ROI placement algorithm has not failed due to anatomic variability, motion, or other processing failures.

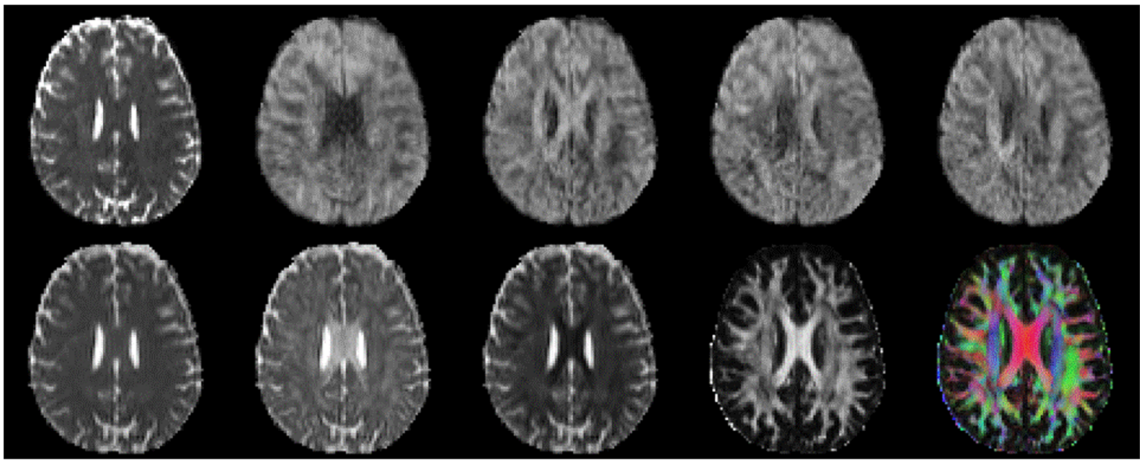

Fig. 5 Example DTI data from a healthy subject. DTI scan parameters 2 mm isotropic resolution, TR = 8500 ms, TE = 90 ms, 30 diffusion volumes with b = 1000 and 6 volumes with b = 0, two averages, scan time = 11 min. *Top row* shows b = 0 s/mm^2 scan followed by 4 different slices with b = 1000 s/mm^2 and different gradient orientations. *Bottom row* mean diffusivity, axial diffusivity, radial diffusivity, fractional anisotropy, tensor color map

Histogram Analysis

In a histogram analysis the full range for a particular DTI metric is divided into discrete bins and a count is performed within a region of interest to determine the number of voxels with parameter values that fall within the range of each bin. A histogram analysis can be used to look for subtle changes that impact large areas or the entirety of the brain. Numeric characteristics of the histogram such as peak location, mean, median as well as more complex representations of the histogram shape (Dehmeshki et al. 2001) can then be compared between groups. Histogram analyses can be sensitive to diffuse effects, have less need for manual intervention, and provide fewer tests (hence a lower correction for multiple comparisons). Drawbacks include a lack of anatomic specificity, selecting an appropriate bin size, normalization, and smoothing level, decisions on how to handle partial volume voxels and the care needed to remove tissue of non-interest (CSF, WM, Lesion, artifact, etc). As with manual ROI placement, histogram analysis is less common now than in the past.

Voxel Based Method

The voxel based method (VBM) analysis approach is a common method to analyze MRI data. Originally developed for structural imaging (Ashburner and Friston 2000), it was quickly used in DTI analysis (Foong et al. 2002). In a voxel based approach subject images are registered to a common template space. Individual anatomy is distorted to achieve a voxel-wise correspondence across subjects. A statistical analysis is then performed voxel-wise to uncover group differences or correlations between DTI metrics and descriptor variables for the study populations.

The image processing for a VBM analysis usually includes computation of the scalar map of interest (i.e. FA or MD) in the data acquisition space, registration of the data to a common template space and spatial smoothing. Once the parametric maps are registered to a common location, statistical analysis is performed on the resultant data on a voxel-wise basis using multiple regression or similar methods followed by significance testing. Multiple comparison corrections must be performed on the resulting maps to reduce the type-1 error because of the large number of voxels in the image space. Both parametric and non-parametric methods can be used for correction.

VBM methods are frequently used for DTI analyses. Because VBM is automated, the methods have the potential to be highly reproducible and scalable to large study samples. VBM also allows for testing across the whole brain while providing high anatomical specificity. VBM results can have a strong dependence on the details of the steps used in the analysis pipeline, i.e. the template chosen, the smoothing level used, the methods for image registration and the methods used to correct for multiple comparisons. In particular, the automated registration methods may fail, in some cases spectacularly, resulting in misregistration of the anatomy and possibly faulty conclusions. Checking each registration will guard against this error. Other concerns include the level of interpolation needed in these registrations, which invariably lead to partial voluming, the high significance level needed due to overcome the large number of comparisons causing subtle effects to be missed.

Tract Based Spatial Statistics

Tract-based spatial statistics (TBSS) is a type of VBM which is included in the FSL package that is specifically designed for

DTI analyses (Smith et al. 2006). TBSS differs from standard VBM in that it does not require a highly accurate initial registration as with standard VBM but instead uses a template based on a skeletonized fractional anisotropy map that is derived from the nonlinearly aligned FA images of the population being studied. After the skeleton is created, each subject's data is projected on this skeleton and the maximal FA value for each point in the skeleton is determined for the subject. Voxelwise statistics can then be carried out on this skeleton-space FA data.

TBSS is a more sophisticated approach than traditional VBM allowing more precise spatial comparison across subjects, preventing partial volume effects and preventing cross-contamination of different tissues (Peng et al. 2014). However, TBSS has some disadvantages. First, TBSS reliability is subject to preprocessing steps choice, see detailed description in Reliability and Validity section (Madhyastha et al. 2014). Second, as with other purely DTI based methods TBSS does not allow proper estimation of diffusion in voxels where there are crossing tracts or junctions (Smith et al. 2006). Third, detection of signal in voxels that are farther away from tract centers is reduced because they have lower contribution to the average of voxels projected to that tract location (Smith et al. 2006). Fourth, when regions are located exactly between two skeleton points, they can be split into two locations when projected to nearest skeleton (Zalesky 2011)(de Groot et al. 2013; Keihaninejad et al. 2012)(Schwarz et al. 2014) Schwarz and colleagues (Schwarz et al. 2014) propose modifications to the TBSS standard pipeline that maximize (de Groot et al. 2013; Keihaninejad et al. 2012) through the use of groupwise registration based on Advanced Normalization Tools (ANTS; (Avants et al. 2008)) or alternate non-linear registration algorithms that exclude the skeleton projection step.

Tractography

In addition to producing scalar metrics of diffusion, the tensor model also produces voxel-wise information of the local orientation of the primary diffusion vector, which for white matter is assumed to be the direction of the dominant fiber bundle. Tractography pieces together this directional information to infer physical connectivity among brain regions. Diffusion tractography is currently the only noninvasive, in vivo method for studying structural brain connectivity. Various methods have developed that vary based on the approach taken of how to connect the vectors and what other information is used. Deterministic tractography was the first tractography approach described (Mori et al. 1999), it involves reconstruction of a white matter tract by selecting a seed starting point and following a streamline based on the preferred direction of diffusion ellipsoids until an ending criteria is reached and the entire pathway is delineated. A disadvantage of the deterministic tractography is that because the resolution of dMRI measurements (voxel size) is much larger than an axon, there are typically thousands of axons passing through a given voxel, and they may not all go in the same direction (Wiegell et al. 2000). Although individual axons are usually organized into large bundles containing thousands of axons that are coherently organized to connect the same basic brain regions, these fiber bundles cross each other, split or merge with one another, or fan out as they reach gray matter structures. To help overcome the limitations caused by multiple fiber orientations in a voxel as well as the effects effects of measurement noise, probabilistic tractography was developed. In probabilistic tractography, most likely fiber orientations are estimated at each voxel along with the probability distribution that a fiber would run along these directions. These probability distributions are then used to trace thousands of probable connections based on slightly jittered orientations (Behrens et al. 2003). The resulting set of probable paths constitute a measure of the connection probability. Examples of packages that have deterministic tractography options are FACT (Fiber Assignment by Continuous Tracking (Mori et al. 1999), AFNI (3dTrackID http://afni.nimh.nih.gov/pub/dist/doc/program_help/3dTrackID.html), CAMINO (http://cmic.cs.ucl.ac.uk/camino/), DTIStudio (Jiang et al. 2006) and TrackVis (http://trackvis.org/). Examples of packages that have options for probabilistic tractography are FSL (http://fsl.fmrib.ox.ac.uk/fsl/fslwiki), TRACULA (https://surfer.nmr.mgh.harvard.edu/fswiki/Tracula), CAMINO, AFNI (3dTrackID http://afni.nimh.nih.gov/pub/dist/doc/program_help/3dTrackID.html).

Figure 6 shows an example of how diffusion tractography can be used to estimate the paths of 18 specific white matter tracts by using the TRACULA package (Yendiki et al. 2011). Tracula combines global probabilistic tractography methods from FSL and prior distributions on the neighboring anatomical structures of each pathway derived from an atlas and a FreeSurfer cortical parcellation and subcortical segmentation of the subject that is being analyzed to constrain the tractography solutions. TRACULA is automated and eliminates user interaction (e.g., to manually drawn seed ROIs or threshold setting on path angle and length). TRACULA has been used to identify ROIs relevant to neuropsychiatric disease being studied (Lee et al. 2015; Wozniak et al. 2014). Figure 7 shows an example of how DSI Studio (http://dsi-studio.labsolver.org/) software can be used to estimate white matter streamlines from diffusion MRI data acquired under the Human Connectome Project (HCP; WU-Minn Consortium (Sotiropoulos et al. 2013; Van Essen et al. 2012)). DSI Studio uses a generalized deterministic fiber tracking algorithm with quantitative anisotropy to generate tractography maps (Fang-Cheng et al. 2014).

Finally, diffusion tractography can also be used to generate subject specific connectivity matrices of the brain. Just as a connectivity matrices can be constructed from functional connectivity among brain regions, measures of anatomical

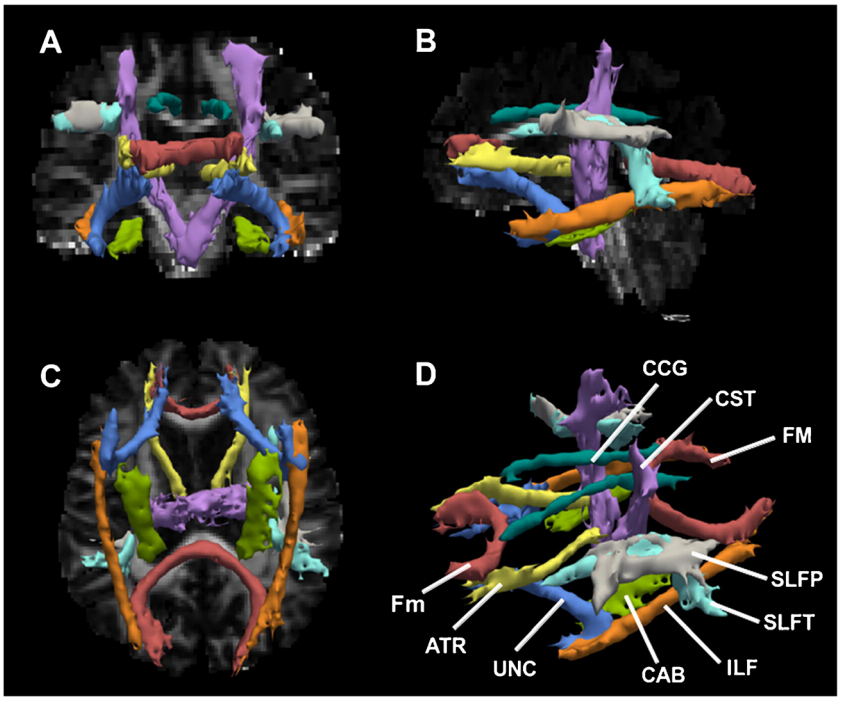

Fig. 6 Radiological views of the 18 reconstructed white matter tracts overlaid on fractional anisotropy map in a control participant [coronal (**a**), sagittal (**b**) and axial (**c**)], and 3D anatomical view (**d**). CCG = cingulum-cingulate gyrus bundle; CST = corticospinal tract; FM = corpus callosum-forceps major; Fm = corpus callosum-forceps minor; SLFP = superior longitudinal fasciculus-parietal endings; SLFT = superior longitudinal fasciculus-temporal endings; ILF = inferior longitudinal fasciculus; CAB = cingulum-angular bundle; UNC = uncinate fasciculus; ATR = anterior thalamic radiations (reprinted from (Lee et al. 2015) with permission)

connectivity from tractography (.e.g. number of streamlines, probabilistic connections) can also be used to construct anatomical connectivity matrices. Graph theoretical approaches can then be used to quantify network properties such as clustering coefficient, path length, degree distribution, modularity, centrality, hubs and efficiency (Bullmore and Sporns 2009; van den Heuvel et al. 2008). Graph theory analysis on dMRI data has provided evidence of disrupted topological

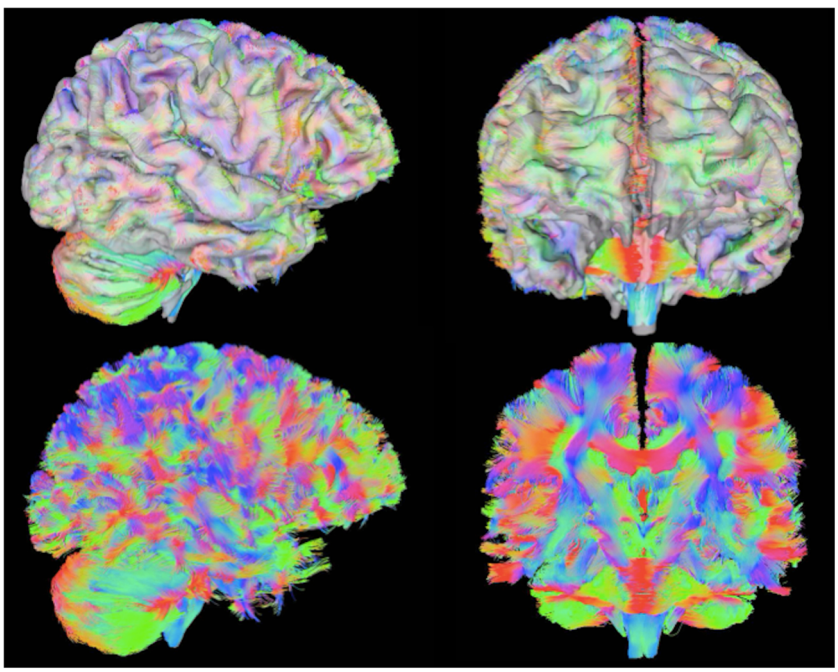

Fig. 7 Example of whole brain tractography using 3 T diffusion MRI data. The streamline color code (DSI studio; http://dsi-studio.labsolver.org/) indicates local fiber orientation (red: left-right; green: anterior-posterior; blue: inferior-superior). The surface approximates the boundary white/grey matter and was obtained by thresholding the fractional anisotropy (FA) map. *Top left*: side view with cortical surface; *Bottom left*: side view with cortical surface removed revealing tractography streamlines; *Top right*: frontal view with cortical surface; *Bottom right*: coronal slice through corpus callosum. Data from the Human Connectome Project (HCP), WU-Minn Consortium (Principal Investigators: David Van Essen and Kamil Ugurbil; 1U54MH091657) funded by the 16 NIH Institutes and Centers that support the NIH Blueprint for Neuroscience Research; and by the McDonnell Center for Systems Neuroscience at Washington University

organization of white matter networks in brain disorders (Cao et al. 2013; Ottet et al. 2013b; Vecchio et al. 2015).

Beyond Tensor

Many dMRI studies to date have been interpreted using the tensor model. DTI has proven to be an invaluable method for discovering information about the underlying microstructure of the brain, particularly in the white matter. Among the model assumptions are that, on a per voxel basis, the underlying structure is comprised of a single compartment with hindered but not restricted diffusion which obeys a three dimensional Gaussian distribution over time (Basser and Jones 2002). This model, however, is known to be incorrect, even in the most simple case of a voxel containing just a single bundle of parallel axons (e.g. in the corpus callosum), the tissue consists of two different water compartments: one compartment inside the axons (where water is mostly restricted to stay within the axon itself) and one extracellular compartment around the axons (where water is hindered by axonal boundaries but not prevented from diffusing over distances many times the axonal diameter). Further, at least on the 2 mm scale of a typical dMRI voxel, up to 90 % of the brain white matter may not be well modeled as a single collection of parallel axons (Jeurissen et al. 2013). Early in the development of dMRI it was realized that more sophisticated models are needed to better describe the complex architecture of the brain's white matter, with several water pools and where within-voxel fiber crossing, fanning, "kissing", or bending are common.

Recent technological advances in scanner hardware, pulse sequences, reconstruction methods, computer speeds, and analysis methods have been developed to make the use of diffusion models beyond DTI practical in large scale human imaging studies. The evolution in diffusion imaging is most clearly demonstrated by the efforts of the NIH funded Human Connectome Project (Sotiropoulos et al. 2013). A major advance has been acceleration of imaging acquisition using simultaneous multi-slice EPI with multiband (MB) excitation and multiple receivers, enabling acceleration of diffusion data acquisition by a factor of 3 or more. This acceleration has made the collection of the additional data needed for non DTI models clinically feasible.

So many alternatives to the tensor model of diffusion have been proposed over the past 20 years that a comprehensive listing is well beyond the scope of this paper. All the beyond the tensor model descriptions include additional fitting parameters, most require additional diffusion volumes and/or acquisition of diffusion data with more and/or higher b values.

DSI

Perhaps the most complete model is diffusion spectral imaging (DSI). The goal of DSI is to completely characterize the probability diffusion function (PDF) at each voxel. The PDF is the diffusion probability distribution as a function of distance and direction of water in each voxel (Basser and Pajevic 2002; Rathi and Westin 2015; Tuch et al. 2003). A measurement of the PDF provides a fairly complete description of water diffusion in the brain, however there are limitations to this methodology. First, a DSI acquisition requires collecting diffusion data with high angular sampling (lots of diffusion directions) with a large range of b values sampled using an equal lattice spacing, requiring many hundreds of diffusion volumes (Tuch et al. 2003). Even with recent advances in imaging and analysis methods such acquisitions may not be practical for most clinical populations, although DSI has been successfully used in a few cases.

HARDI

High angular resolution diffusion imaging (HARDI) is the name given to a diffusion acquisition with high angular sampling in the diffusion direction. The exact criteria for classifying a dMRI acquisition as a HARDI acquisition is not consistent in the literature, but an acquisition with many directions (from 60 to 250+) and a single, higher b value, in which the diffusion signal has a much lower contribution for isotropic diffusion, are typically used as a criteria. High angular sampling allows for the application of models beyond DTI to extract orientation diffusion function (ODF), the probability distribution for water diffusion in a given direction without regard to the magnitude of the diffusion. The ODF can then be evaluated to look for multiple peaks in diffusion probability, which are then labeled as distinct fiber bundles within the voxel. Fiber tracking algorithms which account for voxels identified with two or more crossing fibers can then be used to track through such areas. Many such analysis methods have been used on HARDI data including spherical harmonic deconvolution (Hess et al. 2006; Tournier et al. 2004), generalized diffusion tensor imaging (Ozarslan and Mareci 2003), and q-ball (Tuch 2004) imaging.

Diffusion Kurtosis Imaging (DKI)

Kurtosis is a dimensionless statistic that quantifies the "peakedness" or deviation from a Gaussian of a distribution. Diffusion kurtosis imaging (DKI) is an extension of DTI that parametrizes the kurtosis, i.e. deviations from a Gaussian distribution of the diffusion probability distribution function (Jensen et al. 2005). A distribution with a positive kurtosis will have a sharper peaked and higher tails while a negative kurtosis will have a flatter peak and lower tails compared to a Gaussian distribution with the same variance. Early in the

development of diffusion imaging diffusion signal loss was observed to deviated from linearity as a function of diffusion b value (Niendorf et al. 1994, 1996). The deviations was believed explained as resulting from there being two water pool compartments in the voxel with fast and slow diffusion properties. The kurtosis model is just including the second order term in the expression of the log of the signal loss as the cumulant expansion in powers of the diffusion b value (Jensen et al. 2005):

$$\ln\left(S(b)\Big/S(0)\right) = -b{\cdot}D + 1\Big/6{\cdot}b^2{\cdot}D^2{\cdot}K + 0\left(b^3\right)$$

where $\boldsymbol{S}(b)$ is the signal with diffusion encoding b, D is the apparent diffusion coefficient (ADC), K is the apparent diffusion kurtosis, and $O\left(b^3\right)$ are higher order terms in the expansion.

The kurtosis model includes the next rank tensor to the diffusion modeling, the rank 4 (3×3×3×3) tensor K in addition to the rank 2 (3 × 3) diffusion tensor D. Because both tensors are fully symmetric with respect to an interchange of indices, however, only 6 components in the DTI tensor and 15 components in the DKI tensor are independent (Jensen and Helpern 2010). From the kurtosis computation many rotationally invariant scalar metrics can be computed. All the voxel-wise scalar parameters computed from the DTI model including axial, radial and mean diffusivity as well as fractional anisotropy can be derived from the DKI fit, however the modeling should be more accurate because the explicit nonlinear diffusion change is properly modeled in the fit. In addition, several new measures can be derived, including mean kurtosis (MK - the average diffusion kurtosis in all directions), axial kurtosis (AK - the kurtosis along the axial direction of the diffusion ellipsoid), and radial kurtosis (RK - the kurtosis along the radial direction) (Jensen and Helpern 2010).

A DKI imaging acquisition is relatively simple to implement on most clinical DTI capable MRI scanners, however the DKI model requires at least three b values including one high b value (e.g. b = 0 s/mm^2, 800 s/mm^2, 2600 s/mm^2 (Yan et al. 2013)) with at least 15 independent diffusion gradient direction per diffusion shell (Jensen and Helpern 2010). This requirement does increase the time needed to acquire a DKI compared to a DTI data set. Figure 8 shows the parametric maps of a diffusion data set reconstructed using DKI methods. Recent improvements in scanner hardware and software and improved analysis methods have allowed many brain imaging studies that have used DKI have been published in the literature.

CHARMED

The composite hindered and restricted model of diffusion (CHARMED) is an expansion of the DTI methodology that relates the measured signal to biophysical measures in the tissue compartment (Assaf and Basser 2005; Assaf et al. 2004). The assumption in the CHARMED model is that white matter contains two independent pools: the axonal space in which restricted diffusion takes place and extracellular space in which hindered diffusion takes place. Separating the contribution of restricted diffusion from diffusion of the other compartments provides for a better characterization of the axonal water compartment. The CHARMED model parametrizes the diffusivity of the hindered component (the non-axonal pool), the volume fraction and the fiber directions of the restricted component (axonal pool). While the CHARMED approach has the potential to offer improved characterization of white matter in clinical populations, to our knowledge this method has not been applied to clinical populations to date. This is likely caused by the need to acquire diffusion data over a wide range of b values (up to 10, 000 s/mm^2) and along many diffusion directions, requiring a protocol that takes an increased acquisition time. A recent study has shown that by using an optimized sampling scheme it is possible to reduce acquisition times sufficient for clinical studies (Santis et al. 2014).

NODDI

Neurite orientation dispersion and density imaging (NODDI) is a diffusion MRI technique for estimating the microstructural complexity of dendrites and axons in vivo (Jelescu et al. 2015; Zhang et al. 2012). This technique builds on the work of Alexander (2008) and requires diffusion data with high angular resolution with at least two shells but is achievable in a clinical setting. A typical NODDI MRI sequence acquires whole-brain images with 2 mm (isotropic) voxels resolution in around 25 min although the scanning time can be shorter (e.g. 10 min scan) if the angular resolution is reduced. Information provided by the orientation and dispersion of white matter allows the quantification of spatial distribution (bending and fanning) of axons which describes the quality of brain connectivity (Fig. 8). One limitation of the method is that model fits only cylindrical axons, with particularly compromised accuracy of orientation distribution in regions where there is fanning and axon crossing. Nevertheless, with optimized parameters, NODDI provides the ability to examine density and orientation of neurites in the whole brain using a clinical scanner with clinically feasible scanning times.

Reliability and Validity

The clinical applicability of this brain architecture metric relies on the ability to generate reproducible findings that are scanner-independent, and inherently site-independent. One method used to test for quality assurance and reproducibility

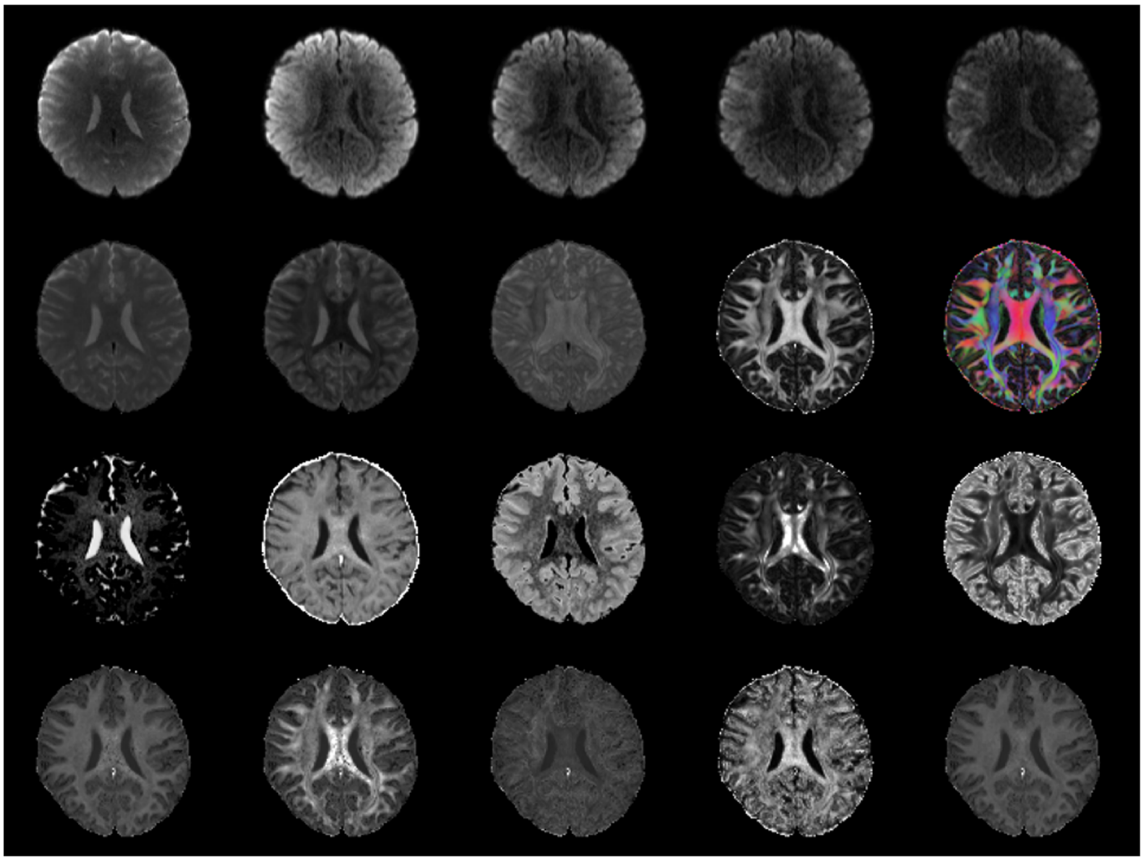

Fig. 8 Diffusion and parametric maps from a high resolution, MB-DTI, multi-shell data set. Scan parameters include MB = 3, 1.5 mm isotropic resolution, TR = 3300 ms, TE = 68 ms, 30 diffusion directions and 4 b = 0 s/mm^2 volumes per shell, shells with b = 1000, 1500, 2000, 2500 s/mm^2, image time = 8:30 per scan. Two data sets were acquired with with opposite phase encode directions then merged together using the FSL tool eddy. *Top row* shows b = 0, 1000, 1500, 2000, 2500 s/mm^2 volumes from the same gradient direction. *Second row* parametric maps of MD, RD, AD, FA, and FA color map computed using tensor model. *Third row* contains parametric maps fit using the NODDI toolkit (http://mig.cs.ucl.ac.uk/index.php?n=Tutorial.NODDImatlab), isotropic volume fraction (fiso), the intracellular volume fraction (ficvf), the extracellular volume fraction (fec), the concentration parameter of the Watson distribution (kappa), and the orientation dispersion index (ODI). The f*ourth row* contains parametric maps from DKI fit to the data from the DKE toolkit (http://academicdepartments.musc.edu/cbi/dki/dke.html), mean kurtosis (kmean), radial kurtosis (krad), axial kurtosis (kax), kurtosis fractional anisotropy (kfa), and kurtisos mean (mkt)

of diffusion weighted imaging data across sites is the use of phantoms. Phantoms eliminate subject variability and allows examination of scanner quality and acquisition reproducibility. For example, Belli and colleagues (Belli et al. 2015) recently conducted a large-scale study in which a standard doped water phantom was scanned at 26 different center sites with standard acquisition protocols and standardized instructions for investigators. They reported that more than 80 % of mean apparent diffusion coefficient (ADC) measurements were within 5 % from the nominal value and the highest deviation from this mean was 9.3 % (overall SD = 3.5 %). Their findings suggest that reliability of diffusion weighted imaging data can be attained if acquisition protocols and instructions are standardized across studies or sites.

Reliability in data acquisition is also essential for longitudinal studies in which the research topic involves examining white matter changes over time to understand disease trajectory or to monitor therapeutic effects in clinical samples. While longitudinal data acquisition requires consideration of additional sources of variance such as MRI system instabilities, variability in head position in relation to the head coil and operator differences, there are reports in the literature of test-retest reproducibility in longitudinal studies. For example, Jovicich and colleagues (Jovicich et al. 2014) evaluated the test-retest and multi-site reliability of DTI tract-based spatial statistics taken from ten clinical 3 T MRI sites. They found good test-retest reliability on a variety of metrics and produced values consistent with those reported in fewer sites, supporting the conclusion that adding testing sites is not necessarily a source of increased noise/decreased reliability. Reliability of data acquisition parameters proposed by the Human Connectome Project have been examined with intra-class correlation coefficients (ICCs) suggesting higher reliability for (i) first order metrics (vs. second order metrics) when examining global network properties; (ii) volume-based parcellation (vs. surface-based parcellation); (iii) high-

resolution (vs. low resolution) when examining global metrics; (iv) low-resolution (vs. high resolution) when examining local metrics; (v) association and primary cortices (vs. limbic and paralimbic regions); hubs (vs. non-hubs); and multiband acquired data (vs. conventional dMRI sequences) (Zhao et al. 2015).

Reliability of white matter integrity metrics (FA, MD, AD, RD) also needs to be considered. In general, there is evidence of high test-retest reliability for these metrics (most ICCs in the 0.9+ range). However, reliability seems to be associated (i) with spatial location within the brain so that limbic and cingulum tracts both have shown lower reliability (ICC of 0.7+) and (ii) with age so that greater variability and poor reliability for tract volume measurements is found in younger patients such as in pediatric epilepsy patients (as low as ICCs 0.5+) (Carlson et al. 2014).

dMRI Reliability may also vary depending on the adopted analysis approach. For example, there is evidence that tract-based methods have better reproducibility and test-retest reliability than ROIs (Brandstack et al. 2014). A study that evaluated the reliability of identified white matter tracts from diffusion MRI data collected at two separate scans used a variety of combinations of data analyses including (i) two alternative tractography algorithms (deterministic tensor tractography (FACT (Mori et al. 1999)) and probabilistic algorithm modeling (FDT BedpostX/ProbtrackX (Behrens et al. 2003, 2007))); (ii) two alternative seeding approaches (white-matter and gray-matter seeding); and (iii) three types of network weighting were recorded for each set of streamlines, two based on streamline density and a third on tract-averaged FA (Buchanan et al. 2014). Buchanan and colleagues found that network metric reproducibility can be improved by using probabilistic (not deterministic) methods, seeding from the white matter (rather than gray matter), and selecting streamline density weighting (not streamline density weighting with length correction) (Buchanan et al. 2014).

dMRI Reliability can also be affected by the choice of data processing steps. Madhyastha et al. (Madhyastha et al. 2014) cautioned that small preprocessing choices can have significant effects on test-retest reliability. They examined reliability of different preprocessing steps included in TBSS: (i) the use of a subject-specific (vs common individual template); (ii) motion correction, eddy current correction, and tensor estimation using either the FSL pipeline or the DTIPrep pipeline (Liu et al. 2010); (iii) noise removal with DTIPrep; and (iv) smoothing using either 1 voxel median filter (GTRACT; (Magnotta et al. 2012)) or 1 voxel box kernel (FSL fslmaths). After comparison of different preprocessing steps, Madhyastha and colleagues (Madhyastha et al. 2014) reported that two pre-processing steps improve TBSS reliability by systematically increasing the number of voxels in the skeleton that overlapped within an individual subject (increasing reliability by improving within-subject skeleton alignment): 1) the use of a common individual template and 2) smoothing a 1-voxel median filter.

While post-mortem diffusion imaging data is useful to investigate ex vivo white matter integrity in humans, there is evidence that reliability of diffusion properties of postmortem DTI samples degrades over time (Miller et al. 2011). Although diffusion anisotropy may still be detected in the major white matter tracts as late as a post-mortem interval (PMI) of 14 days, regional FA and ADC values in mice (4.7 T) quickly declined with increasing PMI, as did the number of and coherence of reconstructed fiber pathways (D'Arceuil and de Crespigny 2007).

There are two main factors that affect reliability and validity of dMRI studies: data collection and data processing. In order to maximize reliability and validity, selection of scanning parameters needs to be carefully considered keeping in mind that the goal is to maximize efficiency of data collection aiming for the best signal to noise ratio. DMRI acquisition parameters for individual sites are determined by hardware and software platform.

The review of scanning parameters based on individual platform differences is beyond the scope of the current manuscript. However, one general principle to maximize signal is to reduce echo time (TE; time between application of radiofrequency exCitation pulse and the peak of the signal induced in the coil) to improve signal to noise ratio. Echo time is often limited by strength of gradients and how fast can these gradients change. Guidelines for proper data collection using parameters compatible with the Human Connectome Project can be found in (Setsompop et al. 2013). Once the most optimal scanning parameters are selected, the stability of scanner is paramount for high data quality collection. Echo-planar imaging (EPI) is the most common image acquisition used in MRI, including dMRI. There has been extensive work in developing stability monitoring for EPI particularly for fMRI scanning protocols (Friedman and Glover 2006). Such quality assurance procedures include regular measurements (preferably weekly assessments) of signal-to-noise ratio (SNR), signal-to-fluctuation-noise ratio (SFNR), percent fluctuation, and drift to evaluate scanner performance periodically (Friedman and Glover 2006). While Marcus and colleagues (Marcus et al. 2013) provide standard quality control guidelines for structural and functional MRI data collection, a standard quality control for dMRI data has not been implemented yet (currently under construction). A final recommendation to maximize reliability and validity under data collection is that data from different groups should be collected contemporaneously to avoid systematic differences in scanner state.

Regarding analysis issues that may affect reliability and validity, factors such as susceptibility-induced distortions, transformations during correction of eddy current distortions, motion correction, estimation of the tensor, voxel-wise quantitative parameters, anisotropy bias, orientation encoding,

extraction of quantitative parameters, corticospinal fluid contamination, data normalization, smoothing, group difference sensitivity, statistical analyses, and skeletonization are covered extensively (Jones and Cercignani 2010). Jones and cercignani (Jones and Cercignani 2010) identify several "pitfalls" related to the above factors, and provide recommendations to address these potential issues that may affect reliability and validity.

Areas of use and Work in Clinical Samples

Disruption of brain anatomical connectivity can result in alterations of brain function underlying psychiatric clinical symptoms and poor cognition. Diffusion weighted imaging is particularly useful for the examination of white matter integrity of long-range tracts making it valuable to examine brain functional architecture in psychiatric conditions that have been related either to localized disruptions in brain connectivity (e.g. ischaemic damage) or disrupted global connectivity (e.g. schizophrenia and autism). The first clinical use of dMRI was for detection of ischaemic damage (Sevick et al. 1990). Sevick and colleagues (1990) reported that the signal provided by diffusion weighted images can be used to define the anatomic locus of ischaemic damage better than T_2-weighted images. dMRI data was identified as an imaging modality for early detection and accurate localization of ischaemic changes in stroke patients. Since this early study, dMRI has been useful for diagnosing, measuring disease severity, determining stages of the disease, and monitoring progression in patients with ischaemic stroke (Roldan-Valadez and Lopez-Mejia 2014; Simonsen et al. 2015; Uno et al. 2015).

Schizophrenia, a disorder characterized by the disconnection or lack of integration of thought processes, was the first psychiatric disorder to be explored with dMRI. One of the first studies that identified white matter integrity alterations in schizophrenia patients reported widespread lower fractional anisotropy in schizophrenia patients when compared to controls despite groups having similar white matter volumes (Lim et al. 1999). More localized alterations have since been identified in schizophrenia patients ranging from lower white matter integrity in the corpus callosum, particularly the frontal portions (Kubicki et al. 2003; Sun et al. 2003; Wang et al. 2004) to disruption in identified tracts such as the uncinate fasciculus and cingulum bundle (Fujiwara et al. 2007; Voineskos et al. 2010). A global approach to the examination of brain connectivity in schizophrenia can be conducted by examining connectivity in predetermined nodes at the whole-brain level (Zalesky et al. 2011). By using whole-brain tractography, Zalesky and colleagues (Zalesky et al. 2011) identified specific pairs of nodes between which connectivity was lower in the schizophrenia patients vs. controls. Network based statistics specifically identified lower connection between a cluster of frontal nodes and a group of parietal and occipital nodes in schizophrenia patients vs. controls via the cingulum bundle and posterior cingulate (Zalesky et al. 2011). While a full consensus on white matter integrity disruptions in schizophrenia patients has not been reached (may be due to scanner, preprocessing, analysis differences, sample variability), there seems to be a general agreement on altered connectivity of networks involving frontal nodes.

Quality of white matter integrity as measured with dMRI has been previously associated with specific behavioral alterations and clinical symptoms in psychiatric disorders (Table 2). In schizophrenia patients, for example, lower fractional anisotropy in right inferior frontal white matter has been correlated with higher motor impulsiveness and aggression (Hoptman et al. 2002, 2004) and with severity of negative symptoms (SANS) such as affective blunting and anhedonia (Wolkin et al. 2003).

Lower fractional anisotropy in white matter regions (uncinate fasciculus, sagittal stratum and superior longitudinal fasciculus) has been associated with severity of symptoms (PANSS) in schizophrenia patients (Michael et al. 2008; Skelly et al. 2008), although recent findings suggest that these relationships may be mediated by age (Bijanki et al. 2015). Nevertheless, the relationship between severity of psychiatric symptoms and quality of white matter integrity has been widely studied in other psychiatric disorders all reporting negative correlations between (i) quality of white matter integrity (lower fractional anisotropy, higher mean diffusivity) in the whole white matter skeleton and severity of traits in autism spectrum disorder (ASD) (Gibbard et al. 2013); (ii) fractional anisotropy (in corpus callosum, cingulate bundle, inferior fronto-occipital fasciculus and right optic radiation) and symptom severity (in the obsessing and ordering dimension) in obsessive compulsive disorder (Koch et al. 2012); (iii) fractional anisotropy (in right superior longitudinal fasciculus) and ADHD (attention deficit hyperactivity disorder) symptom counts (Witt and Stevens 2015); (iv) fractional anisotropy (in fornix and cingulum) and symptom scores (affective instability and anger respectively) in borderline personality disorder (Whalley et al. 2015); and (v) fractional anisotropy (in uncinate fasciculus, inferior fronto-occipital fasciculus, anterior internal capsule) and severity of psychopathy scores in individuals with antisocial personality disorder (Sundram et al. 2012).

The relationship between cognitive performance and white matter integrity has also been examined in psychiatric disorders. For example, a positive correlation has been reported between cognitive performance in tasks that assess attention, memory, executive function and language and fractional anisotropy (attention: cingulate gyrus; memory: fornix/anterior corona radiata; executive function: anterior limb of internal capsule; language: sagittal striatum) in patients with Parkinson's disease (Zheng et al. 2014). Although the relationship between clinical symptoms/cognitive performance and white matter integrity needs to be revisited with more

Table 2 Example of diffusion MRI findings in psychiatric disorders

Disorder	Most Recent dMRI Findings
Addiction (Alcohol Use Disorder)	Longitudinal examination of white matter microstructural integrity found that relapsing individuals with alcohol use disorder had continued worsening, whereas the abstaining individuals showed improvement in DTI indices of fibre integrity (e.g. callosal genu and body; (Pfefferbaum et al. 2014))
Addiction (Stimulant Use Disorder)	Reduced frontal (orbitofrontal, inferior frontal, anterior cingulate) white matter integrity (FA) in individuals with stimulant use disorder (Chung et al. 2007; Lim et al. 2002; Romero et al. 2010)
Alzheimer's Disease	White matter deterioration in fornix, corpus callosum, cingulum, related to cognitive impairments (Daianu et al. 2013; Nir et al. 2013)
Amyotrophic Lateral Sclerosis (ALS)	Upper motor neuron impairment has been examined using diffusion metrics, which have been found to correlate with disease severity and duration (Ellis et al. 1999; Iwata et al. 2008). Can be potentially used for diagnosis, based on reduced FA in corticospinal tract (Liu et al. 2015)
Depression	Disrupted white matter integrity in default mode network and in a network including frontal cortex, thalamus, and caudate (Korgaonkar et al. 2014)
Parkinson's Disease	Full-brain white matter integrity can be used to discriminate between patients and controls (Skidmore et al. 2015). FA within between parkinsonian disorders
Schizophrenia	White matter integrity abnormalities identified in specific regions such as corpus callosum and temporal lobe (Balevich et al. 2015; Ellison-Wright et al. 2014; Lener et al. 2015) Potential trait marker for schizophrenia identified in right arcuate fasciculus of relatives (Skudlarski et al. 2013; Wu et al. 2015)
Stroke	Can be used to monitor outcome: Reduction in lesion volume/complete recovery after 30 days of minor ischemic stroke onset (Kate et al. 2015); white matter damage after ischemic stroke has been related to functional outcomes; degree of recovery related to infarct location (Yassi et al. 2015). Tensor-free approaches allow better detection of damaged tracts than diffusion tensor approaches (Auriat et al. 2015)
Traumatic Brain Injury (TBI)	Reduction in white matter integrity related to mild TBI (e.g. lower FA in internal capsule; (Hayes et al. 2015)) has been found to be proportionally exacerbated with number of blast exposure and loss of consciousness (Hayes et al. 2015; Morey et al. 2013). Post-injury changes in white matter integrity associated with changes in memory and learning can be detected with dMRI (Newcombe et al. 2015)

sophisticated analyses accounting for potential covariates (such as age, gender, medication, substance use), findings from the above mentioned studies suggest an association between brain anatomical organization and clinically relevant behavioral metrics in psychiatric disorders.

Studies have examined white matter integrity in relatives of schizophrenia patients to potentially use this tool as an endophenotype or vulnerability marker of schizophrenia. Findings, however, have not been consistent. While some studies have found reduced fractional anisotropy in relatives of schizophrenia patients when compared to controls (Kang et al. 2012), other have found a potential compensatory mechanism in which relatives of schizophrenia patients have higher fractional anisotropy than healthy controls and schizophrenia patients (Goghari et al. 2014; Kim et al. 2012). It is likely that this inconsistency in white matter integrity alterations relates to the different genetic makeup of schizophrenia relatives, while some may carry similar genetic load as their affected relatives, others may not. A more sophisticated approach that utilizes white matter integrity metrics as potential biomarkers of disease vulnerability has been through the direct use of genotype data as a grouping variable. For example, a study that identified individuals at risk of developing schizophrenia through the presence of the rs1344706 SNP in the ZNF804A gene, found that individuals with this genotype have lower fractional anisotropy in the corpus callosum, left forceps minor, and right parietal white matter, a finding that was related to abnormal myelination (Ikuta et al. 2014). This approach, in which group comparison is based on genotype, is being increasingly used and is a promising development to allow the identification of biomarkers of disease in white matter integrity (Ottet et al. 2013a; Perlstein et al. 2014).

DMRI data can also provide information about disease progression and outcome. For example, while some studies suggest that there is an age-related decline in whole brain fractional anisotropy in schizophrenia patients (Wright et al. 2014), others have not found evidence of this decline when examining white matter tracts (Voineskos et al. 2010). DMRI data can be a useful tool in diseases that affect the central nervous system such as amyotrophic lateral sclerosis (ALS). ALS progression has been found to be correlated to white matter abnormalities identified with dMRI using Q-ball methodologies. Specifically, disease progression has been found to be negatively correlated with tract length and fiber density of corpus callosum in ALS (Caiazzo et al. 2014). In patients with epilepsy, dMRI metrics have been found to be sensitive to transient, progressive and permanent diffusion changes associated with seizure activity in focal and generalized epilepsy,

and detecting post-operational change (Chaudhary and Duncan 2014). In stroke, dMRI has been used to examine white matter changes in patients undergoing rehabilitative motor training. DMRI data collected at three time points (before training, 4- and 8 weeks after training) detected a progressive increase in number and length of fibers in the cortico spinal tract in chronic stroke patients after robotic neurorehabilitation (Lazaridou et al. 2013). In patients with multiple sclerosis, the use of dMRI as a tool that measures outcome for remyelination and repair has been evaluated. While dMRI provides good sensitivity to detecting myelin based changes, it has poor specificity, reproducibility, low SNR, and high susceptibility to motion artifacts (Mallik et al. 2014). The utility of dMRI for examining disease progression and outcome, therefore, needs to be carefully interpreted due to potential confounding variables in observations designed to detect white matter changes across time such as aging, the effect of psychotropics, development of other psychiatric comorbidities, etc.

Given that no single MRI measure is able to provide complete information on brain structure and function, it is best to investigate neural abnormalities in neurologic and neuropsychiatric disorders with a multimodality approach (Chaudhary and Duncan 2014; Chondrogiorgi et al. 2015; Dyrba et al. 2015; Libero et al. 2015; Sui et al. 2015). For example, the utility of dMRI data as a tool for diagnostic evaluation in amyotropic lateral sclerosis (ALS) improves when using a multimodal approach that incorporates dMRI and magnetic resonance spectroscopy (MRS) data, so that data from these two modalities allow the best discrimination between patients with ALS and controls (Area under the receiver operating characteristic curve, AUC 0.93 vs. 0.81) (Foerster et al. 2014).

As to the future, dMRI methods will continue to be used by neuropsychologists and other investigators studying neurological and neuropsychiatric questions. The nature of these studies will continue to improve concurrently with advances in dMRI methods. Hardware and sequences for acquiring dMRI data are constantly evolving with the development of new scanners with faster acquisition (e.g. multiband) that address previously noted shortcomings (Feinberg et al. 2010; Moeller et al. 2010; Zhao et al. 2015). dMRI analysis methods are also evolving from basic tensor models to more sophisticated models that better describe the complex white matter architecture of the brain (e.g DKI (Jensen et al. 2005), CHARMED (Assaf and Basser 2005), NODDI (Zhang et al. 2012), etc.). The ability to examine changes in microstructural complexity may allow for the examination of synaptic plasticity in dMRI studies performed both before and after intervention. For example, the examination of microstructural complexity of dendrites and axons before and after cognitive remediation therapy in schizophrenia patients would allow one to investigate plasticity within networks that potentially mediate executive function deficits characteristic of this disease. Multimodal imaging approaches (that integrate data from different imaging modalities such as MRI, fMRI, dMRI) have begun to be used and have the potential to provide a rich set of information to study neural alterations such as structural (dMRI) and functional (fMRI) connectivity in brain disorders. For example, given that recent findings suggest that interventions for depression result in neurogenesis and synaptogenesis involving restructuring of brain connections (Bambico and Belzung 2013) a combination of neuroimaging methodologies such as dMRI and fMRI can be useful to monitor microstructural and functional network changes related to treatment (e.g. antidepressants or cognitive behavioral therapy) and recovery. The number of subjects included in studies will continue to increase, from tens of subjects per study to hundreds and thousands of subjects per study. The ability to include such large numbers of subjects in a single study will allow for sophisticated analyses which merge genetic and dMRI data into a single analysis. Given the above, multimodal approaches that examine genetics as well as structural and functional connectivity differences and changes related to disease progression, treatment monitoring, and treatment outcome in neuropsychiatric disorders seem to be the future for dMRI research.

Acknowledgments Data for Fig. 8 were provided by the Human Connectome Project, WU-Minn Consortium (Principal Investigators: David Van Essen and Kamil Ugurbil; 1U54MH091657) funded by the 16 NIH Institutes and Centers that support the NIH Blueprint for Neuroscience Research; and by the McDonnell Center for Systems Neuroscience at Washington University. Christophe Lenglet, PhD processed the HCP data.

Center for Magnetic Resonance Imaging (CMRR): P41 EB015894 and P30 NS076408.

Author Funding LH: National Institute on Aging R01AG038651-01A1, National Institute on Aging R01AG386561, National Institute on Aging R01AG039396, National Institute on Aging U01AG046871.

KOL: National Institute on Aging R01AG038651-01A1.

Glossary

MRI	Magnetic resonance imaging - non-invasive technique that provides images of internal structures by measuring excitability of atoms after application of high-frequency radio waves within a strong magnetic field.
EPI	Echo planar imaging - a type of MRI that utilizes only one nuclear spin excitation per scanned image allowing faster acquisitions.
dMRI	Diffusion magnetic resonance imaging - non-invasive technique that measures the diffusion of molecules (mainly water) in biological tissue (such as the

brain) allowing characterization of white matter tracts in the brain.

fMRI Functional magnetic resonance imaging - non-invasive technique that can be used to measure brain activity by detecting changes in blood flow and oxygenation that occur during neural activity.

ASL Arterial spin labeling - non-invasive technique that measures cerebral blood flow (without the need of injection of exogenous tracer) by using water in the blood as an endogenous tracer.

References

Aboitiz, F., Scheibel, A. B., Fisher, R. S., & Zaidel, E. (1992). Fiber composition of the human corpus callosum. *Brain Research*, *598*(1-2), 143–153.

Alexander, D. C. (2008). A general framework for experiment design in diffusion MRI and its application in measuring direct tissue-microstructure features. *Magnetic resonance in medicine: official journal of the Society of Magnetic Resonance in Medicine/Society of Magnetic Resonance in Medicine*, *60*(2), 439–448.

Alexander, A. L., Lee, J. E., Lazar, M., & Field, A. S. (2007). Diffusion tensor imaging of the brain. *Neurotherapeutics: the journal of the American Society for Experimental NeuroTherapeutics*, *4*(3), 316–329.

Ashburner, J., & Friston, K. J. (2000). Voxel-based morphometry–the methods. NeuroImage, 11(6 Pt 1), 805–821.

Assaf, Y., & Basser, P. J. (2005). Composite hindered and restricted model of diffusion (CHARMED) MR Imaging of the human brain. *NeuroImage*, *27*(1), 48–58.

Assaf, Y., Freidlin, R. Z., Rohde, G. K., & Basser, P. J. (2004). New modeling and experimental framework to characterize hindered and restricted water diffusion in brain white matter. *Magnetic resonance in medicine: official journal of the Society of Magnetic Resonance in Medicine/Society of Magnetic Resonance in Medicine*, *52*(5), 965–978.

Auriat, A. M., Borich, M. R., Snow, N. J., Wadden, K. P., & Boyd, L. A. (2015). Comparing a diffusion tensor and non-tensor approach to white matter fiber tractography in chronic stroke. *NeuroImage. Clinical*, *7*, 771–781.

Avants, B. B., Epstein, C. L., Grossman, M., & Gee, J. C. (2008). Symmetric diffeomorphic image registration with cross-correlation: evaluating automated labeling of elderly and neurodegenerative brain. *Medical Image Analysis*, *12*(1), 26–41.

Balevich, E. C., Haznedar, M. M., Wang, E., Newmark, R. E., Bloom, R., Schneiderman, J. S., et al. (2015). Corpus callosum size and diffusion tensor anisotropy in adolescents and adults with chizophrenia. *Psychiatry Research*, *231*(3), 244–251.

Bambico, F. R., & Belzung, C. (2013). Novel insights into depression and antidepressants: a synergy between synaptogenesis and neurogenesis? *Current Topics in Behavioral Neurosciences*, *15*, 243–291.

Basser, P. J., & Jones, D. K. (2002). Diffusion-tensor MRI: theory, experimental design and data analysis - a technical review. *NMR in Biomedicine*, *15*(7-8), 456–467.

Basser, P. J., & Pajevic, S. (2002). A normal distribution for tensor-valued random variables to analyze diffusion tensor MRI data. *In Proceedings IEEE International Symposium on Biomedical Imaging* (pp. 927–930). IEEE.

Basser, P. J., Mattiello, J., & LeBihan, D. (1994). MR diffusion tensor spectroscopy and imaging. *Biophysical Journal*, *66*(1), 259–267.

Beaulieu, C. (2002). The basis of anisotropic water diffusion in the nervous system – a technical review. *NMR in Biomedicine*, *15*(7-8), 435–455.

Beaulieu, C. F., Zhou, X., Cofer, G. P., & Johnson, G. A. (1993). Diffusion-weighted MR microscopy with fast spin-echo. *Magnetic resonance in medicine: official journal of the Society of Magnetic Resonance in Medicine/Society of Magnetic Resonance in Medicine*, *30*(2), 201–206.

Behrens, T. E. J., Woolrich, M. W., Jenkinson, M., Johansen-Berg, H., Nunes, R. G., Clare, S., et al. (2003). Characterization and propagation of uncertainty in diffusion-weighted MR imaging. *Magnetic resonance in medicine: official journal of the Society of Magnetic Resonance in Medicine / Society of Magnetic Resonance in Medicine*, *50*(5), 1077–1088.

Behrens, T. E. J., Berg, H. J., Jbabdi, S., Rushworth, M. F. S., & Woolrich, M. W. (2007). Probabilistic diffusion tractography with multiple fibre orientations: What can we gain? *NeuroImage*, *34*(1), 144–155.

Belli, G., Busoni, S., Ciccarone, A., Coniglio, A., Esposito, M., Giannelli, M., et al. (2015). Quality assurance multicenter comparison of different MR scanners for quantitative diffusion-weighted imaging. *Journal of magnetic resonance imaging: JMRI*. doi:10.1002/jmri.24956.

Bijanki, K. R., Hodis, B., Magnotta, V. A., Zeien, E., & Andreasen, N. C. (2015). Effects of age on white matter integrity and negative symptoms in schizophrenia. *Schizophrenia Research*, *161*(1), 29–35.

Brandstack, N., Kurki, T., Laalo, J., Kauko, T., & Tenovuo, O. (2014). Reproducibility of Tract-based and Region-of-Interest DTI Analysis of Long Association Tracts. *Clinical Neuroradiology*. doi:10.1007/s00062-014-0349-8.

Buchanan, C. R., Pernet, C. R., Gorgolewski, K. J., Storkey, A. J., & Bastin, M. E. (2014). Test-retest reliability of structural brain networks from diffusion MRI. *NeuroImage*, *86*, 231–243.

Budde, M. D., Xie, M., Cross, A. H., & Song, S.-K. (2009). Axial diffusivity Is the primary correlate of axonal injury in the experimental autoimmune encephalomyelitis spinal cord: A quantitative pixelwise analysis. Journal of Neuroscience. doi:10.1523/JNEUROSCI.4605-08.2009

Bullmore, E., & Sporns, O. (2009). Complex brain networks: Graph theoretical analysis of structural and functional systems. Nature reviews. Neuroscience, 10(3), 186–198.

Caiazzo, G., Corbo, D., Trojsi, F., Piccirillo, G., Cirillo, M., Monsurrò, M. R., et al. (2014). Distributed corpus callosum involvement in amyotrophic lateral sclerosis: a deterministic tractography study using q-ball imaging. *Journal of Neurology*, *261*(1), 27–36.

Cao, Q., Shu, N., An, L., Wang, P., Sun, L., Xia, M.-R., et al. (2013). Probabilistic diffusion tractography and graph theory analysis reveal abnormal white matter structural connectivity networks in drug-naive boys with attention deficit/hyperactivity disorder. *The Journal of Neuroscience: The Official Journal of the Society for Neuroscience*, *33*(26), 10676–10687.

Carlson, H. L., Laliberté, C., Brooks, B. L., Hodge, J., Kirton, A., Bello-Espinosa, L., et al. (2014). Reliability and variability of diffusion tensor imaging (DTI) tractography in pediatric epilepsy. *Epilepsy & behavior: E&B*, *37*, 116–122.

Chang, L.-C., Jones, D. K., & Pierpaoli, C. (2005). RESTORE: Robust estimation of tensors by outlier rejection. *Magnetic resonance in medicine: official journal of the Society of Magnetic Resonance in Medicine/Society of Magnetic Resonance in Medicine*, *53*(5), 1088–1095.

Chaudhary, U. J., & Duncan, J. S. (2014). Applications of blood-oxygen-level-dependent functional magnetic resonance imaging and diffusion tensor imaging in epilepsy. *Neuroimaging Clinics of North America*, *24*(4), 671–694.

Chavez, S., Storey, P., & Graham, S. J. (2009). Robust correction of spike noise: application to diffusion tensor imaging. *Magnetic resonance in medicine: official journal of the Society of Magnetic Resonance in Medicine/Society of Magnetic Resonance in Medicine*, *62*(2), 510–519.

Chondrogiorgi, M., Tzarouchi, L. C., Zikou, A. K., Astrakas, L. G., Kosta, P., Argyropoulou, M. I., & Konitsiotis, S. (2015). Multimodal imaging evaluation of excessive daytime sleepiness in Parkinson's disease. *The International Journal of Neuroscience*, 1–17.

Chung, A., Lyoo, I. K., Kim, S. J., Hwang, J., Bae, S. C., Sung, Y. H., et al. (2007). Decreased frontal white-matter integrity in abstinent methamphetamine abusers. *The international journal of neuropsychopharmacology / official scientific journal of the Collegium Internationale Neuropsychopharmacologicum*, *10*(6), 765–775.

D'Arceuil, H., & de Crespigny, A. (2007). The effects of brain tissue decomposition on diffusion tensor imaging and tractography. *NeuroImage*, *36*(1), 64–68.

Daianu, M., Jahanshad, N., Nir, T. M., Toga, A. W., Jack Jr., C. R., Weiner, M. W., et al. (2013). Breakdown of brain connectivity between normal aging and Alzheimer's disease: a structural k-core network analysis. *Brain Connectivity*, *3*(4), 407–422.

De Groot, M., Vernooij, M. W., Klein, S., Ikram, M. A., Vos, F. M., Smith, S. M., et al. (2013). Improving alignment in tract-based spatial statistics: evaluation and optimization of image registration. *NeuroImage*, *76*, 400–411.

Dehmeshki, J., Ruto, A. C., Arridge, S., Silver, N. C., Miller, D. H., & Tofts, P. S. (2001). Analysis of MTR histograms in multiple sclerosis using principal components and multiple discriminant analysis. *Magnetic resonance in medicine: official journal of the Society of Magnetic Resonance in Medicine/Society of Magnetic Resonance in Medicine*, *46*(3), 600–609.

Dubois, J., Kulikova, S., Hertz-Pannier, L., Mangin, J.-F., Dehaene-Lambertz, G., & Poupon, C. (2014). Correction strategy for diffusion-weighted images corrupted with motion: application to the DTI evaluation of infants' white matter. *Magnetic Resonance Imaging*, *32*(8), 981–992.

Dyrba, M., Grothe, M., Kirste, T., & Teipel, S. J. (2015). Multimodal analysis of functional and structural disconnection in Alzheimer's disease using multiple kernel SVM. *Human Brain Mapping*, *36*(6), 2118–2131.

Einstein, A. (1926). Investigations on the theory of the Brownian movement. (R. Furth, Ed.). Dover Publications, Inc.

Ellis, C. M., Simmons, A., Jones, D. K., Bland, J., Dawson, J. M., Horsfield, M. A., et al. (1999). Diffusion tensor MRI assesses corticospinal tract damage in ALS. *Neurology*, *53*(5), 1051–1058.

Ellison-Wright, I., Nathan, P. J., Bullmore, E. T., Zaman, R., Dudas, R. B., Agius, M., et al. (2014). Distribution of tract deficits in chizophrenia. *BMC Psychiatry*, *14*, 99.

Fang-Cheng, Y., Verstynen, T. D., Yibao, W., Fernández-Miranda, J. C., & Tseng, W.-Y. I. (2014). Deterministic diffusion fiber tracking improved by quantitative anisotropy. *PloS One*, *9*(1). doi:10.1371/annotation/0f3b12de-8b8b-4dda-9ff4-835b8631e1dc.

Feinberg, D. A., Moeller, S., Smith, S. M., Auerbach, E., Ramanna, S., Gunther, M., et al. (2010). Multiplexed echo planar imaging for subsecond whole brain FMRI and fast diffusion imaging. *PloS One*, *5*(12), e15710.

Foerster, B. R., Carlos, R. C., Dwamena, B. A., Callaghan, B. C., Petrou, M., Edden, R. A. E., et al. (2014). Multimodal MRI as a diagnostic biomarker for amyotrophic lateral sclerosis. *Annals of Clinical and Translational Neurology*, *1*(2), 107–114.

Foong, J., Symms, M. R., Barker, G. J., Maier, M., Miller, D. H., & Ron, M. A. (2002). Investigating regional white matter in schizophrenia using diffusion tensor imaging. *Neuroreport*, *13*(3), 333–336.

Friedman, L., & Glover, G. H. (2006). Report on a multicenter fMRI quality assurance protocol. *Journal of magnetic resonance imaging: JMRI*, *23*(6), 827–839.

Fujiwara, H., Namiki, C., Hirao, K., Miyata, J., Shimizu, M., Fukuyama, H., et al. (2007). Anterior and posterior cingulum abnormalities and their association with psychopathology in schizophrenia: a diffusion tensor imaging study. *Schizophrenia Research*, *95*(1-3), 215–222.

Gallichan, D., Scholz, J., Bartsch, A., Behrens, T. E., Robson, M. D., & Miller, K. L. (2010). Addressing a systematic vibration artifact in diffusion-weighted MRI. *Human Brain Mapping*, *31*(2), 193–202.

Gibbard, C. R., Ren, J., Seunarine, K. K., Clayden, J. D., Skuse, D. H., & Clark, C. A. (2013). White matter microstructure correlates with autism trait severity in a combined clinical–control sample of high-functioning adults. *NeuroImage: Clinical*, 3(0), 106–114.

Glover, G. H., Mueller, B. a, Turner, J. a, van Erp, T. G. M., Liu, T. T., Greve, D. N., et al. (2012). Function biomedical informatics research network recommendations for prospective multicenter functional MRI studies. *Journal of magnetic resonance imaging: JMRI*, 36(1), 39–54.

Goghari, V. M., Billiet, T., Sunaert, S., & Emsell, L. (2014). a diffusion tensor imaging family study of the fornix in schizophrenia. *Schizophrenia Research*, *159*(2-3), 435–440.

Gudbjartsson, H., Maier, S. E., Mulkern, R. V., Mórocz, I. A., Patz, S., & Jolesz, F. A. (1996). Line scan diffusion imaging. *Magnetic resonance in medicine: official journal of the Society of Magnetic Resonance in Medicine/Society of Magnetic Resonance in Medicine*, *36*(4), 509–519.

Hayes, J. P., Miller, D. R., Lafleche, G., Salat, D. H., & Verfaellie, M. (2015). The nature of white matter abnormalities in blast-related mild traumatic brain injury. *NeuroImage. Clinical*, *8*, 148–156.

Hess, C. P., Mukherjee, P., Han, E. T., Xu, D., & Vigneron, D. B. (2006). Q-ball reconstruction of multimodal fiber orientations using the spherical harmonic basis. *Magnetic resonance in medicine: official journal of the Society of Magnetic Resonance in Medicine/Society of Magnetic Resonance in Medicine*, *56*(1), 104–117.

Hoptman, M. J., Volavka, J., Johnson, G., Weiss, E., Bilder, R. M., & Lim, K. O. (2002). Frontal white matter microstructure, aggression, and impulsivity in men with schizophrenia: a preliminary study. *Biological Psychiatry*, *52*(1), 9–14.

Hoptman, M. J., Ardekani, B. A., Butler, P. D., Nierenberg, J., Javitt, D. C., & Lim, K. O. (2004). DTI and impulsivity in schizophrenia: a first voxelwise correlational analysis. *Neuroreport*, *15*(16), 2467–2470.

Hua, K., Zhang, J., Wakana, S., Jiang, H., Li, X., Reich, D. S., et al. (2008). Tract probability maps in stereotaxic spaces: analyses of white matter anatomy and tract-specific quantification. *NeuroImage*, *39*(1), 336–347.

Ikuta, T., Peters, B. D., Guha, S., John, M., Karlsgodt, K. H., Lencz, T., et al. (2014). A schizophrenia risk gene, ZNF804A, is associated with brain white matter microstructure. *Schizophrenia Research*, *155*(1-3), 15–20.

Iwata, N. K., Aoki, S., Okabe, S., Arai, N., Terao, Y., Kwak, S., et al. (2008). Evaluation of corticospinal tracts in ALS with diffusion tensor MRI and brainstem stimulation. *Neurology*, *70*(7), 528–532.

Jelescu, I. O., Veraart, J., Adisetiyo, V., Milla, S. S., Novikov, D. S., & Fieremans, E. (2015). One diffusion acquisition and different white matter models: How does microstructure change in human early development based on WMTI and NODDI? *NeuroImage*, *107*, 242–256.

Jellison, B. J., Field, A. S., Medow, J., Lazar, M., Salamat, M. S., & Alexander, A. L. (2004). Diffusion tensor imaging of cerebral white matter: a pictorial review of physics, fiber tract anatomy, and tumor imaging patterns. *AJNR. American Journal of Neuroradiology*, *25*(3), 356–369.

Jensen, J. H., & Helpern, J. A. (2010). MRI quantification of non-Gaussian water diffusion by kurtosis analysis. *NMR in Biomedicine*, *23*(7), 698–710.

Jensen, J. H., Helpern, J. A., Ramani, A., Lu, H., & Kaczynski, K. (2005). Diffusional kurtosis imaging: The quantification of non-gaussian water diffusion by means of magnetic resonance imaging. *Magnetic resonance in medicine: official journal of the Society of*

Magnetic Resonance in Medicine/Society of Magnetic Resonance in Medicine, *53*(6), 1432–1440.

Jeurissen, B., Leemans, A., Tournier, J.-D., Jones, D. K., & Sijbers, J. (2013). Investigating the prevalence of complex fiber configurations in white matter tissue with diffusion magnetic resonance imaging. *Human Brain Mapping*, *34*(11), 2747–2766.

Jiang, H., van Zijl, P. C. M., Kim, J., Pearlson, G. D., & Mori, S. (2006). DtiStudio: resource program for diffusion tensor computation and fiber bundle tracking. *Computer Methods and Programs in Biomedicine*, *81*(2), 106–116.

Jones, D. K., & Cercignani, M. (2010). Twenty-five pitfalls in the analysis of diffusion MRI data. *NMR in Biomedicine*, *23*(7), 803–820.

Jovicich, J., Marizzoni, M., Bosch, B., Bartrés-Faz, D., Arnold, J., Benninghoff, J., et al. (2014). Multisite longitudinal reliability of tract-based spatial statistics in diffusion tensor imaging of healthy elderly subjects. *NeuroImage*, *101*, 390–403.

Kang, Z., Wei, Q.-L., Tang, Y.-X., Li, L.-J., Zheng, L.-R., Guo, X.-F., et al. (2012). Diffusion tensor imaging analyses of white matter in healthy siblings of schizophrenics. *Zhonghua Yi Xue Za Zhi*, *92*(39), 2772–2774.

Kate, M. P., Riaz, P., Gioia, L., Sivakumar, L., Jeerakathil, T., Buck, B., et al. (2015). Dynamic Evolution of Diffusion-Weighted Imaging Lesions in Patients With Minor Ischemic Stroke. *Stroke; a journal of cerebral circulation*. doi:10.1161/STROKEAHA.115.009775.

Keihaninejad, S., Ryan, N. S., Malone, I. B., Modat, M., Cash, D., Ridgway, G. R., et al. (2012). The importance of group-wise registration in tract based spatial statistics study of neurodegeneration: a simulation study in Alzheimer's disease. *PloS One*, *7*(11), e45996.

Kim, S. N., Park, J. S., Jang, J. H., Jung, W. H., Shim, G., Park, H. Y., et al. (2012). Increased white matter integrity in the corpus callosum in subjects with high genetic loading for schizophrenia. *Progress in Neuro-Psychopharmacology & Biological Psychiatry*, *37*(1), 50–55.

Koch, K., Wagner, G., Schachtzabel, C., Schultz, C. C., Straube, T., Güllmar, D., et al. (2012). White matter structure and symptom dimensions in obsessive-compulsive disorder. *Journal of Psychiatric Research*, *46*(2), 264–270.

Korgaonkar, M. S., Fornito, A., Williams, L. M., & Grieve, S. M. (2014). Abnormal structural networks characterize major depressive disorder: a connectome analysis. *Biological Psychiatry*, *76*(7), 567–574.

Kubicki, M., Westin, C.-F., Nestor, P. G., Wible, C. G., Frumin, M., Maier, S. E., et al. (2003). Cingulate fasciculus integrity disruption in schizophrenia: a magnetic resonance diffusion tensor imaging study. *Biological Psychiatry*, *54*(11), 1171–1180.

Lazaridou, A., Astrakas, L., Mintzopoulos, D., Khanicheh, A., Singhal, A. B., Moskowitz, M. A., et al. (2013). Diffusion tensor and volumetric magnetic resonance imaging using an MR-compatible hand-induced robotic device suggests training-induced neuroplasticity in patients with chronic stroke. *International Journal of Molecular Medicine*, *32*(5), 995–1000.

Le Bihan, D. (2003). Looking into the functional architecture of the brain with diffusion MRI. *Nature reviews. Neuroscience*, 4(6), 469–480.

Le Bihan, D., Mangin, J. F., Poupon, C., Clark, C. A., Pappata, S., Molko, N., & Chabriat, H. (2001). Diffusion tensor imaging: concepts and applications. *Journal of magnetic resonance imaging: JMRI*, *13*(4), 534–546.

LeBihan, D. (1990). IVIM method measures diffusion and perfusion. *Diagnostic imaging*, *12*(6), 133, 136.

Lee, A. T., Glover, G. H., & Meyer, C. H. (1995). Discrimination of large venous vessels in time-course spiral blood-oxygen-level-dependent magnetic-resonance functional neuroimaging. *Magnetic resonance in medicine: official journal of the Society of Magnetic Resonance in Medicine/Society of Magnetic Resonance in Medicine*, *33*(6), 745–754.

Lee, S.-H., Coutu, J.-P., Wilkens, P., Yendiki, A., Rosas, H. D., Salat, D. H., & Alzheimer's disease Neuroimaging Initiative (ADNI). (2015). Tract-based analysis of white matter degeneration in Alzheimer's isease. *Neuroscience*, 301(0), 79–89.

Lener, M. S., Wong, E., Tang, C. Y., Byne, W., Goldstein, K. E., Blair, N. J., et al. (2015). White matter abnormalities in schizophrenia and schizotypal personality disorder. *Schizophrenia Bulletin*, *41*(1), 300–310.

Libero, L. E., DeRamus, T. P., Lahti, A. C., Deshpande, G., & Kana, R. K. (2015). Multimodal neuroimaging based classification of autism spectrum disorder using anatomical, eurochemical, and white matter orrelates. *Cortex; a journal devoted to the study of the nervous system and behavior*, *66*, 46–59.

Lim, K. O., Hedehus, M., Moseley, M., de Crespigny, A., Sullivan, E. V., & Pfefferbaum, A. (1999). Compromised white matter tract integrity in schizophrenia inferred from diffusion tensor maging. *Archives of General Psychiatry*, *56*(4), 367–374.

Lim, K. O., Choi, S. J., Pomara, N., Wolkin, A., & Rotrosen, J. P. (2002). Reduced frontal white matter integrity in cocaine dependence: a controlled diffusion tensor imaging study. *Biological Psychiatry*, *51*(11), 890–895.

Liu, Z., Wang, Y., Gerig, G., Gouttard, S., Tao, R., Fletcher, T., & Styner, M. (2010). Quality control of diffusion weighted images. *Proceedings of SPIE The international society for optical engineering*, *7628*. doi:10.1117/12.844748

Liu, C., Jiang, R., Yi, X., Zhu, W., & Bu, B. (2015). Role of diffusion tensor imaging or magnetic resonance spectroscopy in the diagnosis and disability assessment of amyotrophic lateral sclerosis. *Journal of the Neurological Sciences*, *348*(1-2), 206–210.

Madhyastha, T., Mérillat, S., Hirsiger, S., Bezzola, L., Liem, F., Grabowski, T., & Jäncke, L. (2014). Longitudinal reliability of tract-based spatial statistics in diffusion tensor imaging. *Human Brain Mapping*, *35*(9), 4544–4555.

Magnotta, V. A., Matsui, J. T., Liu, D., Johnson, H. J., Long, J. D., Bolster Jr., B. D., et al. (2012). Multicenter reliability of diffusion tensor imaging. *Brain Connectivity*, *2*(6), 345–355.

Mallik, S., Samson, R. S., Wheeler-Kingshott, C. A. M., & Miller, D. H. (2014). Imaging outcomes for trials of remyelination in multiple sclerosis. *Journal of Neurology, Neurosurgery, and Psychiatry*, *85*(12), 1396–1404.

Marcus, D. S., Harms, M. P., Snyder, A. Z., Jenkinson, M., Wilson, J. A., Glasser, M. F., et al. (2013). Human connectome project informatics: quality control, database services, and data visualization. *NeuroImage*, *80*, 202–219.

Michael, A. M., Calhoun, V. D., Pearlson, G. D., Baum, S. A., & Caprihan, A. (2008). Correlations of diffusion tensor imaging values and symptom scores in patients with schizophrenia. *Conference proceedings: ... Annual International Conference of the IEEE Engineering in Medicine and Biology Society. IEEE Engineering in Medicine and Biology Society. Conference*, *2008*, 5494–5497.

Miller, K. L., Stagg, C. J., Douaud, G., Jbabdi, S., Smith, S. M., Behrens, T. E. J., et al. (2011). Diffusion imaging of whole, post-mortem human brains on a clinical mri scanner. *NeuroImage*, *57*(1), 167–181.

Moeller, S., Yacoub, E., Olman, C. A., Auerbach, E., Strupp, J., Harel, N., & Uğurbil, K. (2010). Multiband multislice GE-EPI at 7 tesla, with 16-fold acceleration using partial parallel imaging with application to high spatial and temporal whole-rain fMRI. *Magnetic resonance in medicine: official journal of the Society of Magnetic Resonance in Medicine/Society of Magnetic Resonance in Medicine*, *63*(5), 1144–1153.

Mohammadi, S., Nagy, Z., Hutton, C., Josephs, O., & Weiskopf, N. (2012). Correction of vibration artifacts in DTI using phase-encoding eversal (COVIPER). *Magnetic resonance in medicine: official journal of the Society of Magnetic Resonance in Medicine/Society of Magnetic Resonance in Medicine*, *68*(3), 882–889.

Morey, R. A., Haswell, C. C., Selgrade, E. S., Massoglia, D., Liu, C., Weiner, J., et al. (2013). Effects of chronic mild traumatic brain

injury on white matter integrity in Iraq and Afghanistan war veterans. *Human Brain Mapping*, *34*(11), 2986–2999.

Mori, S., Crain, B. J., Chacko, V. P., & van Zijl, P. C. (1999). Three-dimensional tracking of axonal projections in the brain by magnetic resonance maging. *Annals of Neurology*, *45*(2), 265–269.

Moseley, M. E., Cohen, Y., Kucharczyk, J., Mintorovitch, J., Asgari, H. S., Wendland, M. F., et al. (1990). Diffusion-weighted MR imaging of anisotropic water diffusion in cat central nervous system. *Radiology*, *176*(2), 439–445.

Newcombe, V. F. J., Correia, M. M., Ledig, C., Abate, M. G., Outtrim, J. G., Chatfield, D., et al. (2015). Dynamic changes in white matter abnormalities correlate with late improvement and deterioration following TBI: A Diffusion Tensor Imaging Study. *Neurorehabilitation and neural repair*. doi:10.1177/1545968315584004

Niendorf, T., Norris, D. G., & Leibfritz, D. (1994). Detection of apparent restricted diffusion in healthy rat brain at short diffusion times. *Magnetic resonance in medicine: official journal of the Society of Magnetic Resonance in Medicine/Society of Magnetic Resonance in Medicine*, *32*(5), 672–677.

Niendorf, T., Dijkhuizen, R. M., Norris, D. G., van Lookeren Campagne, M., & Nicolay, K. (1996). Biexponential diffusion attenuation in various states of brain tissue: implications for diffusion-weighted imaging. *Magnetic resonance in medicine: official journal of the Society of Magnetic Resonance in Medicine/Society of Magnetic Resonance in Medicine*, *36*(6), 847–857.

Nir, T. M., Jahanshad, N., Villalon-Reina, J. E., Toga, A. W., Jack, C. R., Weiner, M. W., et al. (2013). Effectiveness of regional DTI measures in distinguishing Alzheimer's disease, MCI, and normal aging. *NeuroImage. Clinical*, *3*, 180–195.

Nolte, U. G., Finsterbusch, J., & Frahm, J. (2000). Rapid isotropic diffusion mapping without susceptibility artifacts: Whole brain studies using diffusion-weighted single-shot STEAM MR imaging. *Magnetic resonance in medicine: official journal of the Society of Magnetic Resonance in Medicine/Society of Magnetic Resonance in Medicine*, *44*(5), 731–736.

O'Donnell, L. J., & Westin, C.-F. (2011). An introduction to diffusion tensor image analysis. *Neurosurgery Clinics of North America*, *22*(2), 185–196 viii.

Ottet, M.-C., Schaer, M., Cammoun, L., Schneider, M., Debbané, M., Thiran, J.-P., & Eliez, S. (2013a). Reduced fronto-temporal and limbic connectivity in the 22q11.2 deletion syndrome: vulnerability markers for developing schizophrenia? *PloS one*, *8*(3), e58429.

Ottet, M.-C., Schaer, M., Debbané, M., Cammoun, L., Thiran, J.-P., & Eliez, S. (2013b). Graph theory reveals dysconnected hubs in 22q11DS and altered nodal efficiency in patients with hallucinations. *Frontiers in Human Neuroscience*, *7*, 402.

Ozarslan, E., & Mareci, T. H. (2003). Generalized diffusion tensor imaging and analytical relationships between diffusion tensor imaging and high angular resolution diffusion imaging. *Magnetic resonance in medicine: official journal of the Society of Magnetic Resonance in Medicine/Society of Magnetic Resonance in Medicine*, *50*(5), 955–965.

Peng, S.-J., Harnod, T., Tsai, J.-Z., Huang, C.-C., Ker, M.-D., Chiou, J.-C., et al. (2014). Through diffusion tensor magnetic resonance imaging to evaluate the original properties of neural pathways of patients with partial seizures and secondary generalization by individual anatomic reference atlas. *BioMed esearch international*, *2014*, 419376.

Perlstein, M. D., Chohan, M. R., Coman, I. L., Antshel, K. M., Fremont, W. P., Gnirke, M. H., et al. (2014). White matter abnormalities in 22q11.2 deletion syndrome: preliminary associations with the Nogo-66 receptor gene and symptoms of sychosis. *Schizophrenia Research*, *152*(1), 117–123.

Pfefferbaum, A., Rosenbloom, M. J., Chu, W., Sassoon, S. A., Rohlfing, T., Pohl, K. M., et al. (2014). White matter microstructural recovery with abstinence and decline with relapse in alcohol dependence interacts with normal geing: a controlled longitudinal DTI tudy. *The Lancet Psychiatry*, *1*(3), 202–212.

Pipe, J. G., Farthing, V. G., & Forbes, K. P. (2002). Multishot diffusion-weighted FSE using PROPELLER MRI. *Magnetic resonance in medicine: official journal of the Society of Magnetic Resonance in Medicine/Society of Magnetic Resonance in Medicine*, *47*(1), 42–52.

Rathi, Y., & Westin, C.-F. (2015). Probability distribution functions in diffusion MRI. In *Brain Mapping* (pp. 253–255). Elsevier.

Roldan-Valadez, E., & Lopez-Mejia, M. (2014). Current concepts on magnetic resonance imaging (MRI) perfusion-diffusion assessment in acute ischaemic stroke: a review & an update for the linicians. *The Indian Journal of Medical Research*, *140*(6), 717–728.

Romero, M. J., Asensio, S., Palau, C., Sanchez, A., & Romero, F. J. (2010). Cocaine addiction: diffusion tensor imaging study of the inferior frontal and anterior cingulate white matter. *Psychiatry Research*, *181*(1), 57–63.

Santis, S., Assaf, Y., Evans, C. J., & Jones, D. K. (2014). Improved precision in CHARMED assessment of white matter through sampling scheme optimization and model parsimony testing. *Magnetic resonance in medicine: official journal of the Society of Magnetic Resonance in Medicine/Society of Magnetic Resonance in Medicine*, *71*(2), 661–671.

Schwarz, C. G., Reid, R. I., Gunter, J. L., Senjem, M. L., Przybelski, S. A., Zuk, S. M., et al. (2014). Improved DTI registration allows voxel-based analysis that outperforms tract-based spatial tatistics. *NeuroImage*, *94*, 65–78.

Setsompop, K., Kimmlingen, R., Eberlein, E., Witzel, T., Cohen-Adad, J., McNab, J. A., et al. (2013). Pushing the limits of in vivo diffusion MRI for the Human Connectome Project. *NeuroImage*, *80*, 220–233.

Sevick, R. J., Kucharczyk, J., Mintorovitch, J., Moseley, M. E., Derugin, N., & Norman, D. (1990). Diffusion-weighted MR imaging and T2-weighted MR imaging in acute cerebral ischaemia: comparison and correlation with histopathology. *Acta Neurochirurgica. Supplementum*, *51*, 210–212.

Simonsen, C. Z., Madsen, M. H., Schmitz, M. L., Mikkelsen, I. K., Fisher, M., & Andersen, G. (2015). Sensitivity of diffusion- and perfusion-weighted imaging for diagnosing acute ischemic troke is 97.5 %. *Stroke; a journal of cerebral circulation*, *46*(1), 98–101.

Skelly, L. R., Calhoun, V., Meda, S. A., Kim, J., Mathalon, D. H., & Pearlson, G. D. (2008). Diffusion tensor imaging in schizophrenia: relationship to symptoms. *Schizophrenia Research*, *98*(1-3), 157–162.

Skidmore, F. M., Spetsieris, P. G., Anthony, T., Cutter, G. R., von Deneen, K. M., Liu, Y., et al. (2015). A full-brain, bootstrapped analysis of diffusion tensor imaging robustly differentiates Parkinson disease from healthy controls. *Neuroinformatics*, *13*(1), 7–18.

Skudlarski, P., Schretlen, D. J., Thaker, G. K., Stevens, M. C., Keshavan, M. S., Sweeney, J. A., et al. (2013). Diffusion tensor imaging white matter endophenotypes in patients with schizophrenia or psychotic bipolar disorder and their relatives. *The American Journal of Psychiatry*, *170*(8), 886–898.

Smith, S. M., Jenkinson, M., Johansen-Berg, H., Rueckert, D., Nichols, T. E., Mackay, C. E., et al. (2006). Tract-based spatial statistics: voxelwise analysis of multi-subject diffusion data. *NeuroImage*, *31*(4), 1487–1505.

Song, S.-K., Sun, S.-W., Ramsbottom, M. J., Chang, C., Russell, J., & Cross, A. H. (2002). Dysmyelination revealed through MRI as increased radial (but unchanged axial) diffusion of water. *NeuroImage*, *17*(3), 1429–1436.

Sotiropoulos, S. N., Jbabdi, S., Xu, J., Andersson, J. L., Moeller, S., Auerbach, E. J., et al. (2013). Advances in diffusion MRI acquisition and processing in the Human Connectome Project. *NeuroImage*, *80*, 125–143.

Stejskal, E. O., & Tanner, J. E. (1965). Spin diffusion measurements: spin echoes in the presence of a time-dependent field gradient. *The Journal of Chemical Physics*, *42*(1), 288–292.

Sui, J., Pearlson, G. D., Du, Y., Yu, Q., Jones, T. R., Chen, J., et al. (2015). In search of multimodal neuroimaging biomarkers of cognitive deficits in schizophrenia. *Biological Psychiatry*. doi:10.1016/j.biopsych.2015.02.017.

Sun, Z., Wang, F., Cui, L., Breeze, J., Du, X., Wang, X., et al. (2003). Abnormal anterior cingulum in patients with schizophrenia: a diffusion tensor imaging tudy. *Neuroreport*, 14(14), 1833–1836.

Sundram, F., Deeley, Q., Sarkar, S., Daly, E., Latham, R., Craig, M., et al. (2012). White matter microstructural abnormalities in the frontal lobe of adults with antisocial personality disorder. *Cortex; a journal devoted to the study of the nervous system and behavior*, *48*(2), 216–229.

Tournier, J.-D., Calamante, F., Gadian, D. G., & Connelly, A. (2004). Direct estimation of the fiber orientation density function from diffusion-weighted MRI data using spherical deconvolution. *NeuroImage*, *23*(3), 1176–1185.

Tuch, D. S. (2004). Q-ball imaging. *Magnetic resonance in medicine: official journal of the Society of Magnetic Resonance in Medicine/ Society of Magnetic Resonance in Medicine*, *52*(6), 1358–1372.

Tuch, D. S., Reese, T. G., Wiegell, M. R., & Wedeen, V. J. (2003). Diffusion MRI of complex neural rchitecture. *Neuron*, *40*(5), 885–895.

Uno, H., Nagatsuka, K., Kokubo, Y., Higashi, M., Yamada, N., Umesaki, A., et al. (2015). Detectability of ischemic lesions on diffusion-weighted imaging is biphasic after transient ischemic attack. *Journal of stroke and cerebrovascular diseases: the official journal of National Stroke Association*, *24*(5), 1059–1064.

Van den Heuvel, M. P., Stam, C. J., Boersma, M., & Hulshoff Pol, H. E. (2008). Small-world and scale-free organization of voxel-based resting-state functional connectivity in the human brain. *NeuroImage*, *43*(3), 528–539.

Van Essen, D. C., Ugurbil, K., Auerbach, E., Barch, D., Behrens, T. E. J., Bucholz, R., et al. (2012). The Human Connectome Project: a data acquisition perspective. *NeuroImage*, *62*(4), 2222–2231.

Vecchio, F., Miraglia, F., Curcio, G., Altavilla, R., Scrascia, F., Giambattistelli, F., et al. (2015). Cortical brain connectivity evaluated by graph theory in dementia: a correlation study between functional and structural ata. *Journal of Alzheimer's disease: JAD*, *45*(3), 745–756.

Voineskos, A. N., Lobaugh, N. J., Bouix, S., Rajji, T. K., Miranda, D., Kennedy, J. L., et al. (2010). Diffusion tensor tractography findings in schizophrenia across the adult lifespan. *Brain: A Journal of Neurology*, *133*(Pt 5), 1494–1504.

Vos, S. B., Jones, D. K., Jeurissen, B., Viergever, M. A., & Leemans, A. (2012). The influence of complex white matter architecture on the mean diffusivity in diffusion tensor MRI of the human brain. *NeuroImage*, *59*(3), 2208–2216.

Wang, F., Sun, Z., Cui, L., Du, X., Wang, X., Zhang, H., et al. (2004). Anterior cingulum abnormalities in male patients with schizophrenia determined through diffusion tensor imaging. *The American Journal of Psychiatry*, *161*(3), 573–575.

Whalley, H. C., Nickson, T., Pope, M., Nicol, K., Romaniuk, L., Bastin, M. E., et al. (2015). White matter integrity and its association with affective and interpersonal symptoms in borderline personality disorder. *NeuroImage. Clinical*, *7*, 476–481.

Wiegell, M. R., Larsson, H. B. W., & Wedeen, V. J. (2000). Fiber Crossing in Human Brain Depicted with Diffusion Tensor MR Imaging. *Radiology*, *217*(3), 897–903.

Witt, S. T., & Stevens, M. C. (2015). Relationship between white matter microstructure abnormalities and ADHD symptomatology in adolescents. *Psychiatry Research*, *232*(2), 168–174.

Wolkin, A., Choi, S. J., Szilagyi, S., Sanfilipo, M., Rotrosen, J. P., & Lim, K. O. (2003). Inferior rontal white matter anisotropy and negative symptoms of schizophrenia: a diffusion tensor imaging tudy. *The American Journal of Psychiatry*, *160*(3), 572–574.

Wozniak, J. R., Mueller, B. A., Lim, K. O., Hemmy, L. S., & Day, J. W. (2014). Tractography reveals diffuse white matter abnormalities in Myotonic Dystrophy Type 1. *Journal of the Neurological Sciences*, *341*(1-2), 73–78.

Wright, S. N., Kochunov, P., Chiappelli, J., McMahon, R. P., Muellerklein, F., Wijtenburg, S. A., et al. (2014). Accelerated white matter aging in schizophrenia: role of white matter blood perfusion. *Neurobiology of Aging*, *35*(10), 2411–2418.

Wu, C.-H., Hwang, T.-J., Chen, Y.-J., Hsu, Y.-C., Lo, Y.-C., Liu, C.-M., et al. (2015). Altered integrity of the right arcuate fasciculus as a trait marker of schizophrenia: a sibling study using tractography-based analysis of the whole brain. *Human Brain Mapping*, *36*(3), 1065–1076.

Yan, X., Zhou, M., Ying, L., Yin, D., Fan, M., Yang, G., et al. (2013). Evaluation of optimized b-value sampling schemas for diffusion kurtosis imaging with an application to stroke patient data. *Computerized medical imaging and graphics: the official journal of the Computerized Medical Imaging Society*, *37*(4), 272–280.

Yassi, N., Churilov, L., Campbell, B. C. V., Sharma, G., Bammer, R., Desmond, P. M., et al. (2015). The association between lesion location and functional outcome after ischemic stroke. *International Journal of Stroke: Official Journal of the International Stroke Society*. doi:10.1111/ijs.12537.

Yendiki, A., Panneck, P., Srinivasan, P., Stevens, A., Zöllei, L., Augustinack, J., et al. (2011). Automated probabilistic reconstruction of white-matter pathways in health and disease using an atlas of the underlying natomy. *Frontiers in Neuroinformatics*, *5*, 23.

Zalesky, A. (2011). Moderating registration misalignment in voxelwise comparisons of DTI data: a performance evaluation of skeleton projection. *Magnetic Resonance Imaging*, *29*(1), 111–125.

Zalesky, A., Fornito, A., Seal, M. L., Cocchi, L., Westin, C.-F., Bullmore, E. T., et al. (2011). Disrupted axonal fiber connectivity in chizophrenia. *Biological Psychiatry*, *69*(1), 80–89.

Zhang, H., Schneider, T., Wheeler-Kingshott, C. A., & Alexander, D. C. (2012). NODDI: practical in vivo neurite orientation dispersion and density imaging of the human brain. *NeuroImage*, *61*(4), 1000–1016.

Zhao, T., Duan, F., Liao, X., Dai, Z., Cao, M., He, Y., & Shu, N. (2015). Test-retest reliability of white matter structural brain networks: a multiband diffusion MRI study. *Frontiers in Human Neuroscience*, *9*, 59.

Zheng, Z., Shemmassian, S., Wijekoon, C., Kim, W., Bookheimer, S. Y., & Pouratian, N. (2014). DTI correlates of distinct cognitive impairments in Parkinson's disease. *Human Brain Mapping*, *35*(4), 1325–1333.